ZIP editors for efficient and versatile CRISPR-Cas9 precise genome editing

Thibault C[1], Rosier J[1], Riandière M[1], Marin V[1,2], Fayet S[1], Berges C[1], Espasa R[1], Lamrissi-Garcia I[1], Trian T[3], Bui S[3,4], Dabernat S[1,2], Boutin J[1,2], Moreau-Gaudry F[1,2#*], Bedel A[1,2#*]

1 University of Bordeaux, INSERM, UMR 1312, Bordeaux Institute of Oncology, 146 Rue Léo Saignat, 33076 Bordeaux, France.

2 CHU de Bordeaux, Biochemistry Laboratory, 33000 Bordeaux, France.

3 University of Bordeaux, INSERM, U 1045, Centre de Recherche Cardio-Thoracique de Bordeaux, 33600, Pessac, France

4 Pediatric Cystic Fibrosis Reference Center (CRCM), Bordeaux University Hospital, Hôpital Pellegrin-Enfants, Bordeaux, France.

# equal contribution

* corresponding authors

Abstract

Genome editing technologies create the potential for genetic studies and innovative gene therapies. Here we present new CRISPR-Cas9 tools, named ZIP editors (ZE), loaded with a single-stranded oligodeoxynucleotide (ssODN) template on the Cas ribonucleoprotein complex. The ssODN template is annealed to an extended guide RNA (gRNA) allowing its nuclear delivery at the right place, i.e. the targeted DNA cut, and at the right time. This new template import system is easy-to-design, easy-to-use, inexpensive and very versatile. It increases homology-directed repair (HDR) editing efficiency using Cas9 nuclease as demonstrated at many *loci* in many cell types (up to 12-fold higher HDR editing rate). Based on a heteroduplex gRNA-ssODN, it can also be used with the Cas9 nickase, resulting in HDR editing with minimal InDels, and preventing double-strand break (DSB)-mediated genotoxicity. ZE is a smart easy-to-use non-viral platform adaptable to targeted DSB (high HDR editing efficiency) or nick (high safety) to precisely model and correct a wide range of edits. It is suitable to many biological applications and could be considered for HDR-based gene therapies.

Introduction

The CRISPR-Cas9 system induces DNA double-strand breaks (DSBs) at targeted sites to activate mainly two competitive DNA repair pathways: homology-directed repair (HDR), which allows precise editing with a homologous DNA template, and non-conservative NHEJ/MMEJ pathways, which connect two ends of the broken DNA and are often accompanied by random insertions and deletions (InDels)[1]. The relatively low efficiency of HDR compared to NHEJ/MMEJ repair has been a major hurdle in achieving precise genome editing (PGE) at desired *loci*. Because of their higher efficacy, clinical genome editing protocols have been restricted to imperfect but efficient NHEJ-based approaches. Several techniques have been proposed to obtain a higher PGE rate: i) modulating repair pathways by pharmacological NHEJ/MMEJ inhibition[2–6], by HDR activation *via* the expression of HDR actors[7–9] or Cas9-fusion proteins to enhance the HDR pathway at the targeted *locus*[10–13]; ii) enhancing HDR by S/G2 synchronization[14]; iii) using DSB-less CRISPR tools[15–17]. While promising, these approaches may alter the normal behavior of the targeted cells, raising substantial safety concerns when explored in a therapeutic context[18]. In addition, HDR remains suboptimal. The presence of the exogenous DNA template at the DNA cut is critical for HDR editing. For example, fluorescently labeled donor DNA can be used to enrich cells that are likely to be edited *via* HDR[19,20]. Here, we describe the development of new efficient CRISPR-Cas9 tools, named ZIP editors (ZE), that carry a single-stranded oligodeoxynucleotide (ssODN) template annealed to a modified gRNA allowing ribonucleoprotein (RNP) stability. This specific gRNA-ssODN heteroduplex is very easy-to-design. It does not require any specialized and/or expensive chemical modifications or modified Cas9. The simplicity of using unmodified Cas9, ssODN and easily available modified gRNA makes it readily transferable to all laboratories. Importantly, it is versatile, allowing increased HDR editing efficiency at many *loci*, in cell lines and primary cells with nuclease. Remarkably, this strategy also unlock HDR editing by using safer single nickase.

Results

ZIP editors improve PGE using Cas9 nuclease

To increase the effective concentration of the donor template at the DSB and thus HDR editing efficiency, we developed a strategy to hybridize the ssODN donor template to the gRNA. First, we added a 5'-extension (light green in the schema) on the 80nt ssODN template and a 3'-extension (light pink in the schema) on the gRNA for annealing (Fig. 1a). The RNP complex formed is named ZIP editing 1 (ZE1) and the control RNP with regular free ssODN and gRNA is named UNZIP. To quantify CRISPR-Cas9-mediated genome editing, we used a rapid flow cytometry assay based on eGFP to BFP conversion[21] (Fig. 1b/c). In the case of HDR editing, the substitution of a histidine in place of a tyrosine at position 66 in the chromophore of eGFP shifts its emission toward the blue spectrum[22] (Fig. 1b). HEK293T cells, K562 cells and human foreskin fibroblasts (hFFs) were stably transduced at low multiplicity of infection with a lentiviral construct containing an eGFP/puromycin resistance cassette to obtain less than 10% of $eGFP^+$ cells. After selection, we obtained cells with one copy of eGFP per cell. Reliable simultaneous quantification of HDR- and imprecise-editing was obtained by flow cytometry one week after editing by measuring the appearance of BFP fluorescence or the loss of eGFP fluorescence, respectively (Fig. 1c). The BFP detection is highly specific of HDR editing (no BFP without template). Interestingly, PGE (HDR editing) efficiency was significantly increased by 2-fold with ZE1 compared to UNZIP nucleofection in $eGFP^+$-HEK293T cells (14.9% ± 0.7 *vs* 8% ± 1 respectively, Fig. 1d/e) and was confirmed in an $eGFP^+$-K562 cell line (10.2% ± 3.8 *vs* 5.2% ± 2.6 respectively, Fig. 1f). These data obtained in two cell lines demonstrated that ZIP editing increases PGE by using CRISPR-Cas9 nuclease, with a 2-fold increase in the HDR/InDels ratio.

ZIP editors' improvements

To establish whether ssODN template stability and quantity were critical for PGE, we designed two new ZIP editing systems with either double ssODN hybridization on gRNA or elongated ssODN to slow down its degradation. We named these new systems ZE1D (for Double) and ZE1L (for Long) (Fig. 2a). Elongated hybridized ssODN (ZE1a, 120nt versus 80nt in ZE1, supplementary Fig. S1a) moderately

improved PGE in eGFP$^+$-K562 cells (+26.5%, supplementary Fig. S1b). Because these modifications could affect gRNA stability and Cas9 interaction, we added a t-lock element (orange in the schema) in the second loop of the gRNA, as previously described[23], to reinforce its stability. ZE1L (120nt + t-lock) induced a higher HDR editing rate compared to UNZIP (3-fold increase), to ZE1 (1.7-fold increase, Fig. 2b) and to ZE1a (1.3-fold increase). Importantly, the t-lock element alone did not modify editing efficiency at this target, confirming that a higher ssODN concentration at the DNA break is crucial for PGE (ZE1b, supplementary Fig. S1a/b). We then elongated the ssODN template (170nt, ZE1La, supplementary Fig. S1c/d) and flipped the template with a 3'-extension for hybridization to the gRNA (ZE1Lb, supplementary Fig. S1c/d). However, neither of these constructs improved HDR editing efficiency compared to ZE1L.

To explore whether two tethered templates would improve the HDR editing rate, we designed ZE1D (Fig. 2a) in which ssODNs were each hybridized by a distinct sequence to the gRNA with a t-lock element. ZE1D significantly increased the HDR editing rate in the eGFP$^+$-K562 cell line compared to UNZIP (2.7-fold increase) and to ZE1 (1.4-fold increase, Fig. 2b), but was less efficient than ZE1L. Altogether, ssODN elongation (120nt) associated with a t-lock loop in the gRNA (ZE1L) was the most efficient system, so we named it ZEmax and used it in the following experiments.

Next, we tested ZEmax to edit the *HBB* endogenous locus (Fig. 2c). Because the t-lock element in the gRNA can improve HDR editing efficiency by itself at some *loci*[23], we use the same gRNA (with t-lock stabilization and 3'-extension) as a control in UNZIP2 (Fig. 2d). The only difference between UNZIP2 and ZEmax was the template, i.e. with or without the 5'-extension to anneal (or not) to the gRNA. NGS analysis by Nanopore sequencing across the targeted *HBB* region showed that the seven nucleotides modified in the template were edited with a large 2-fold increase in the HDR editing rate with ZEmax (from around 7 to 13.5%, Fig. 2e). Therefore, ZEmax allowed editing in a wide window from -15 to + 13 bases around the cut site. Then, we evaluated ZE in primary eGFP$^+$-hFFs, which are difficult to edit. ZEmax outperformed the UNZIP control spectacularly by improving HDR editing efficiency up to 12-fold and the HDR/InDels ratio by 16-fold (Fig. 2f).

Another way to increase the HDR/InDels ratio is to mitigate the DNA repair pathways. To date, the most potent molecule to inhibit the NHEJ pathway is AZD7648, a potent inhibitor of DNA PKcs[3]. We decided to challenge ZEmax with this compound. Using eGFP$^+$-hFFs, ZEmax provided a 2-fold higher precise editing efficacy compared to UNZIP with 1 µM AZD7648 exposure (11.1% ± 1.9 *vs* 5.3% ± 1.7 respectively, Fig. 2g). Importantly, a complementary additive effect was observed with the simultaneous use of ZEmax and AZD7648, leading to 16.5 ± 3.7% of HDR-edited cells. Given recent data showing the alarming genotoxicity of AZD7648[24], we decided to use only ZEmax without AZD7648 in the following experiments. To check the versatility of ZIP editing in clinically relevant cells, we evaluated it in cord blood-derived CD34$^+$ hematopoietic stem and progenitor cells (HSPCs) by targeting the exon 4 of *UROS,* an enzyme of the heme biosynthesis (Fig. 2h). In these primary cells, PGE was measured by restriction fragment length polymorphism (RFLP). Digestion occurred after the perfect editing of two nucleotides to create a *SacI* restriction site. The HDR editing rate was more than 2-fold higher with ZEmax than with UNZIP2 (16.5% ± 5.1 *vs* 7.3% ± 4.6 respectively, Fig. 2i).

Taken together, these data showed the high efficacy and versatility of ZEmax in cell lines and primary cells to improve HDR editing efficiency.

***CFTR* gene editing in human pulmonary basal, bronchial and nasal epithelial cells**

We harvested 'healthy' pulmonary epithelial basal cells to model class I nonsense *CFTR* p.(GlyG542Ter), usually named G542X, responsible for cystic fibrosis (NM_000492.4(*CFTR*): c.1624G>T, Fig. 3a). Cells were edited with UNZIP or ZEmax by nucleofection. The template contained i) a non-coding TAG codon to replace the GGA codon (Gly) and ii) a *SacI* restriction site to allow HDR editing analysis by RFLP and mute the PAM to avoid a Cas9 recut. Analysis revealed a 3-fold higher percentage of HDR-edited alleles with the c.1624G>T (G542X) mutation and the other four nucleotides responsible for the *SacI* cut with ZEmax compared to UNZIP, reaching up to 22% (Fig. 3b). We then decided to correct this nonsense mutation, which is not eligible for current pharmacological treatments[25]. We obtained nasal and bronchial epithelial cells from a cystic fibrosis patient with the compound heterozygous G542X mutation. For editing, we used a mutation-specific gRNA targeting

the G542X-mutated allele and a correcting template coding GGA (Gly) instead of TGA (nonsense). We added silent mutations to avoid the Cas9 recut and analyzed editing by Nanopore NGS sequencing (Fig. 3c). Whereas the UNZIP2 system was inefficient to edit these nasal and bronchial epithelial cells, ZEmax allowed moderate complete (7 modifications) HDR editing (Fig. 3d left and right panels, around 2%). Regarding the c.1624T>G correction, cells were initially 50% c.1624G. We obtained around 56 or 57 % of c.1624G after editing, i.e. 6 or 7% of genomic edition in bronchial and nasal epithelial cells, respectively (Fig. 3e). This result, which is higher than for other substitutions, suggests an additive pathway to correct c.1624T, in accordance with previous reports of gene conversion with the endogenous allele in the event of heterozygosity[26,27].

Cas9 nuclease is known to induce DSB-dependent ON-target genotoxicity[28]. Genome editing with AZD7648 to boost HDR editing causes frequent kilobase- and megabase-scale deletions, chromosome arm loss, and translocations[24]. ZEmax could also modulate genotoxicity. To test this hypothesis, we used our previously published fluorescence-assisted megabase-scale rearrangements detection (FAMReD) system that sensitively detects and quantifies megabase-scale loss-of-heterozygosity[29] (supplementary Fig. S2a). While increasing HDR editing (supplementary Fig. S2b), ZEmax did not increase DSB-dependent megabase-scale LOH frequency compared to UNZIP2 or to gRNA without template (supplementary Fig. S2c). Finally, ZIP editing using Cas9 nuclease increased the PGE rate in many loci and cell types, but InDels and genotoxicity were still present. We thus applied ZE to a DSB-free Cas9 (single Cas9^{D10A} nickase), which is not known to allow HDR editing using RNP transfection.

ZIP editors coupled with Cas9 nickase to obtain PGE

To edit cells without DSB, we applied ZEmax with the t-lock element in the gRNA and a 5'-extended (120nt) ssODN template to Cas9 nickase. The Cas9^{D10A} nickase was preferred as the unmodified HNH domain has higher activity[30] and creates less DSBs[31]. This new system was named ZEN (ZEmax with Nickase, Fig. 4a). As expected, UNZIP with nickase (named UNZEN) with free BFP-ssODN template did not edit eGFP^{+}-HEK293T cells, eGFP^{+}-K562 cells and eGFP^{+}-hFFs or only at very low levels (Fig. 4b),

confirming previous reports showing that it is very difficult to edit the genome using a unique nick[32,33]. Importantly, ZEN induced a 3-fold increase in PGE (BFP^+ cells) in the $eGFP^+$-HEK293T cell line (Fig. 4b, left) and unlocked PGE in the $eGFP^+$-K562 cell line (17-fold increase, Fig. 4b middle) and in primary $eGFP^+$-hFFs (35-fold increase, Fig. 4b right).

To confirm these results, we edited an endogenous locus (*UROS*) in hFFs with a template containing three substitutions (Fig. 4c). To be sure that the difference between UNZEN control and ZEN was really due to the import system and not to other modifications (t-lock or the 3'-extension in the gRNA), we designed a new control with $Cas9^{D10A}$ nickase with a gRNA containing the t-lock element and the 3'-extension, but with a free 120nt template (without 5'-extension, UNZEN2, Fig. 4d). Nanopore sequencing revealed a 4-fold improvement of perfect *UROS* HDR editing (3 concomitant edited bases, Fig. 4e), confirmed by individual base analysis (Fig. 4f) and without any detection of InDels.

Unlike for the nuclease, the absence of InDels using the nickase was an opportunity to repeat editing of the unedited alleles using the same gRNA to enrich the HDR-edited population (Fig. 5a). We made three iterative RNP transfections with ZEN in $eGFP^+$-hFFs and obtained an interesting additive effect leading to more than 3% of BFP^+ cells (Fig. 5b). We confirmed this additive effect targeting *UROS* in hFFs (Fig. 5c).

Then, to take advantage of our easy-to-design ZE tool, we evaluated the impact of the ssODN design and compared two asymmetric templates with either the larger homology arm on the 3'- (ZEN template) or on the 5'-extremity (ZENmax template), relative to the cut site (Fig. 5d). Interestingly, we observed a 2-fold increase in HDR editing in $eGFP^+$-hFFs with ZENmax compared to ZEN (0.71% ± 0.45 *vs* 1.58 ± 0.62 respectively, Fig. 5e). Thus, ZE could be a great help to test and optimize template designs. With ZENmax in $eGFP^+$-hFFs, we confirmed that iterative transfections led to an additive effect and resulted in more than 5% of HDR-edited cells (Fig. 5f).

ZEN can be combined with 'cell state' modulation to increase nick-based HDR editing

To further improve HDR editing efficiency and benefit from the versatility of ZEN, we investigated various pathways known to modulate genome editing. First, we tried to modulate DNA repair pathways. Nick-mediated HDR repair using a single-stranded template is known to be suppressed by RAD51/BRCA2[33]. Thus, we transiently inhibited *BRCA2* using a siRNA in eGFP$^+$-HEK293T cells and eGFP$^+$-K562 cells. In both cell lines, we obtained a spectacular transient drop in *BRCA2* mRNA expression (supplementary Fig. S3a). We achieved a 2-fold increase in HDR editing when BRCA2 was inhibited during editing (supplementary Fig. S3b). However, it was accompanied by a 3 to 4-fold increase in imprecise editing (InDels) in eGFP$^+$-HEK293T cells and eGFP$^+$-K562 cells (supplementary Fig. S3c), probably due to the conversion of nicks into DSBs. Thus, we decided not to pursue the idea of inhibiting *BRCA2* to avoid DSB-associated genotoxicity. We also tried to inhibit *MLH1* by a CRISPR knock-out to modulate the mismatch repair (MMR) pathway, but we encountered toxicity issues after editing (data not shown).

While HDR editing using the Cas9 nuclease is known to depend on the S/G2 phases, the impact of the cell cycle on nick-mediated HDR editing has been less studied[34]. We observed higher HDR editing rates in highly proliferative HEK293T cells than in less proliferative hFFs (Fig. 4b), suggesting that editing could preferentially be performed during the S/G2/M phases. To decipher the role of the cell cycle on HDR-based nick repair, and the S/G2/M phases in particular, we modulated the hFF cell cycle. We used palbociclib, a CDK4/6 inhibitor, to reduce the proportion of eGFP$^+$-hFFs in the S/G2/M phases during editing (Fig. 6a/b). We observed a 2-fold decrease in HDR editing rates (Fig. 6c). In contrast, HDR editing efficiency was improved by almost 2-fold (+85.4%, Fig. 6c) when using the CDK7 inhibitor XL413 during editing to increase the proportion of eGFP$^+$-hFFs in S/G2/M phases (Fig. 6a/b). These data suggest that HDR editing with nickase is S/G2/M phase-dependent.

Chromatin access can also be important for the efficiency of CRISPR tools. We modulated chromatin opening by using HDAC inhibitors in eGFP$^+$-hFFs with ZEN. When we screened several drugs (valproic acid - VPA -, WT-161 and sodium butyrate - NaBut -) at different doses, we observed a global trend

to an increase in HDR editing efficiency in the presence of HDAC inhibitors, and a significant increase with WT-161 at 10 nM (+86.6%), NaBut at 0.3 mM (+52.7%) and more importantly with NaBut at 1 mM (+125%) (Fig. 6d). We validated the effect of NaBut at 1 mM editing *UROS* in hFFs (+81.5%, Fig. 6e).

Therefore, by reaching detectable HDR editing rates at several *loci* and in several cell types with ZEN, we demonstrated that HDR editing with nickase was more efficient during or after replication, and was boosted by HDAC inhibitors and ssODN template design.

Discussion

HDR editing remains a challenge with CRISPR-Cas9, especially for clinical purposes. The spatiotemporal availability of the HDR template at the cut site during repair is supposed to be a key factor for HDR editing. In this study, we explored the import capacity of annealing the ssODN HDR template to the gRNA to increase PGE through DSBs or nicks. Using RNPs, we demonstrated that ZIP editing (ZE) is a ssODN import system very easy to implement and considerably increases HDR editing efficiency. We further optimized ZE for several targets (*eGFP*, *HBB*, *UROS*, *CFTR*, *SORCS1*) in different cell types (HEK293T cells, K562 cells, hFFs, HSPCs and pulmonary, bronchial and nasal epithelial cells) and for various kinds of edits (substitutions and deletions). We obtained up to 12-fold improvement in HDR editing when mediated by a DSB and up to 35-fold when mediated by a single nick compared to a control approach with a free ssODN template.

Other strategies were developed to increase the concentration of the ssODN template near the DNA break. Polymerase-based DNA writing technologies have been developed to produce large template quantities *in situ* near the targeted *locus*. Prime editing enables precise modification of genomes *via* reverse transcription of an RNA pre-template encoded at the 3' end of the gRNA (a prime editor guide RNA, pegRNA) to produce the ssODN template[16]. More recently, a DNA-dependent polymerase-based system known as click editing was developed to amplify the ssODN template with higher fidelity[17,35]. However, these strategies rely on large Cas9 fusion proteins featuring a polymerase

activity whose cell impact remains largely elusive, and they are complex to design and adapt to new targets. Some Cas9 tools have also been developed to directly carry the ssODN template on the RNP complex. ssDODN donors can be tethered to the Cas9 protein *via* the Cas9-avidin biotin-ssODN system[11], the RNP-DNA (RNPD) system[36], the Cas9-PCV system[37], or the Cas9-AeF DBCO-adaptor ssODN system[38]. Alternatively, ssODN can be tethered to the gRNA *via* a S1mplex system and a biotinylated ssODN[39], *via* a chemical link between tracrRNA and the ssODN[20], or directly with the chimeric RNA-DNA donor guide[40]. However, their uses are constrained by chemical synthesis difficulties and risk of destabilizing the Cas9-gRNA interaction. They rely on chemical modifications of the Cas9 protein, fused protein, and/or the ssDNA donor, leading to several drawbacks including complex synthesis, their unsuitability for mRNA-lipid nanoparticle (LNP) and viral delivery systems, the inclusion of additional recombinant proteins, gene therapy immunogenicity, and the increased costs of producing a gene-editing tool. We therefore sought to develop a chemical modification-free approach that can recruit ssDNA donors to the target site and enhance HDR efficiency. Unlike the other approaches, ZE is free from fusion protein or a covalent link between CRISPR-Cas9 components. In this study, we used ZE with ssODN templates shorter than 200nt. However, it would be interesting to use it to import larger double-stranded DNA with a 5'-ssDNA extremity to anneal to the gRNA. This could be a safer non-viral alternative to the AAV or IDLV template currently used for large gene insertions[41].

Importantly, ZE reached high-efficiency HDR editing rates without modulating DNA repair pathways. Indeed, several methods have been proposed to inhibit NHEJ/MMEJ. Small pharmacological molecules (e.g. SCR7, AZD7648, M3814) have been developed to transiently inhibit the NHEJ components (KU70/80, DNA PK, Ligase IV)[2,3]. The concomitant inhibition of NHEJ and MMEJ by polymerase theta (Polθ) inhibitors has also been proposed[4–6]. In all studies, these molecules limit the NHEJ/MMEJ pathways and therefore enhance HDR editing efficiency. Recruitment[7] or ectopic expression of RAD51 alone or combined to SCR7[8,9] can also be used. In the present study, ZE was at least as efficient as AZD7648 to increase the HDR editing rate in hFFs. Interestingly, the efficiency was

improved when ZE and AZD7648 were associated. This combined approach could be interesting to obtain high levels of HDR editing and confirm that the selection of the DSB repair pathway and the recruitment of the DNA template are the two main steps limiting the rate of HDR editing.

However, modulating DNA repair pathways may not be without effect and could alter genome integrity. For example, one of the most potent NHEJ inhibitors, AZD7648, was recently shown to be genotoxic[24], inducing large deletions and translocations. This suggests that DNA repair modulators should be used carefully in clinical studies and that researchers risk misinterpreting the results of mutation modeling, for example. Remarkably, ZE did not increase DSB-associated genotoxicity and HDR editing efficiency in hFFs was higher with ZEmax than with AZD7648 combined with UNZIP. The safety of ZE has to be considered for future clinical applications of CRISPR-Cas9 mediated gene therapy, and ZE has to be preferred to NHEJ inhibitors.

To avoid genotoxicity, editing without DSBs is the grail for gene therapy. However, nick-based editing suffers from a lack of efficiency[42–44] probably due to the involvement of the single-strand break repair (SSBR)[33] and MMR repair pathways. Indeed, it has been described for other SSB-based CRISPR tools, such as base editing[45] and prime editing[46,47] that editing was higher in MLH1-deficient cells and the authors have proposed to inhibit MLH1 (by knock out or using dominant negative) or to trick the MMR pathway with the introduction of a second nick on the opposite strand. However, the latter strategy induces more InDels and ON-target genotoxicity[48]. On the other hand, ZE allowed us to obtain HDR editing without InDels, with a single nickase, and without polymerase or a fusion protein. HDR repair at nicks is known to be influenced by the transcriptional status of the nicked strand (more efficient on the transcribed strand) and suppressed by RAD51/BRCA2 when using a ssDNA template[33]. Here, we confirmed the inhibiting role of BRCA2 on nick-based HDR editing and showed an important increase in imprecise editing, validating BRCA2's importance in maintaining genome integrity[49].

We also investigated the impact of cell cycle modulation on nick-based HDR editing, showing that HDR editing was increased in proliferative cells (synchronized in the S + G2/M phases) and reduced in non-dividing cells (synchronized in the G0/G1 phases). Those results are different from a previous

study done by Zhang, Davis and Maizels in 2021[34] showing that nicks initiated HDR more efficiently in the G1 than in the S/G2 phases. This could be explained by the different cells (primary fibroblasts in this study *vs* HEK293T and U2OS cell lines) and the different methodologies used: pharmacological synchronization of cells in a phase of the cell cycle for 48h *vs* the use of Cas9 fused to degrons, as the previous publication indicated that the G1 phase nicks may persist to be repaired later in cell cycle. We also confirm another important parameter for nick-based HDR editing, the opening of the chromatin, confirming previous studies done with CRISPR-based editing[50,51]. Further studies will be required to improve its efficiency and decipher the nick-based HDR editing mechanisms.

Altogether, ZE is a new programmable chemical-free non-viral versatile tool that can meet the needs of a wide range of experiments. ZEmax based on nuclease is the first choice when a high HDR editing rate is needed and when DSB-associated genotoxicity is acceptable. On the other hand, ZEN tools based on single nickase are more suited when a non-genotoxic approach is required and when low HDR editing efficiency is not an issue, e.g. when iterative editing is feasible. The simplicity of ZE and its versions should extend their utility to the investigation of complex biological issues in a wide range of cells and organisms. Since ZE is modular, it is potentially compatible with several types of template and Cas, so it could play a leading role in many areas of research. Importantly, ZE achieves high HDR editing rates and could be considered to unlock non-viral HDR-based gene therapies.

Methods

Ethical statement

This research complies with all relevant ethical regulations. Human $CD34^+$ HSPCs were isolated from cord blood of healthy donors from Bagatelle Hospital, according to the hospital's ethical institutional review board (Maison de Santé Protestante de Bordeaux, Talence, France) and with the mothers' informed consent.

The patient with cystic fibrosis was recruited at the pediatric cystic fibrosis resource and skills center (CPP 23.00854.000207). Nasal and bronchial epithelial cells were obtained by nasal or bronchial

superficial ciliary brushing, respectively, according to the hospital's ethical institutional review board and with the parents' informed consent.

Control subjects (CPP 23.00854.000207) were recruited after surgical resection at the University Hospital of Bordeaux. Bronchial specimens from all subjects were obtained either by fibroscopic bronchoscopy or lobectomy in macroscopically normal areas, as previously described[52]. All subjects gave their written informed consent to participate in the study after the nature of the procedure had been fully explained.

Cell culture

Human embryonic kidney (HEK) cell line immortalized with large T antigen HEK293T (ATCC®, Manassas, VA, USA) was maintained in Dulbecco's modified Eagle's medium (DMEM), low glucose (1 g/L), L-Glutamine (1 g/L) and pyruvate (Gibco® by Life Technologies™, Carlsbad, USA) supplemented with 10% fetal bovine serum, 100 U/mL penicillin and 100 µg/mL streptomycin (all from Eurobio™, Courtaboeuf, France).

K562 cell line (ATCC®) was maintained in Roswell Park Memorial Institute (RPMI) Medium 1640, L-Glutamine, 25 mM HEPES (Gibco® by Life Technologies™) supplemented with 10% fetal bovine serum (Eurobio™), GlutaMAX (Gibco® by Life Technologies™), 100 U/mL penicillin and 100 µg/mL streptomycin (Eurobio™).

hTERT immortalized human foreskin fibroblasts (hFFs, ATCC®) were maintained in DMEM, high glucose (4.5 g/L), L-Glutamine (1 g/L) and pyruvate (Gibco® by Life Technologies™) supplemented with 10% fetal bovine serum (Eurobio™), 1% essential amino acids (Gibco® by Life Technologies™), 100 U/mL penicillin, 100µg/mL streptomycin (Eurobio™), 10 µg/mL ciprofloxacin (Biogaran™, Colombes, France) and 0.5 µg/mL amphotericin B (Sigma-Aldrich®, Saint Louis, USA). A previously established heterozygous *UROS*$^{+/-}$ hFF cell line was used for the FAMReD genotoxicity assay (see [29] for details).

Human CD34^{+} stem and progenitor cells (HSPCs) were isolated from the cord blood of healthy donors. Briefly, mononuclear cells were isolated by Ficoll gradient. hCD34^{+} cells were purified according to

the manufacturer's instructions (Human CD34-Positive Selection kit II from Stem Cell Technologies, Vancouver, Canada) and purity was analyzed by flow cytometry using phycoerythrin-conjugated anti-CD34 antibody (Biolegend, San Diego, USA). Cryopreserved hCD34$^+$ cells were thawed and cultured in expansion medium consisting in StemSpan SFEM (Stem Cell Technologies) supplemented with Flt3-L (100 ng/mL, Peprotech, Carlsabad, USA), SCF (100 ng/mL Peprotech), human TPO (100 ng/mL Peprotech), vitamin C (0.35 mg/mL, Sigma-Aldrich), ciprofloxacin (10 µg/mL, Biogaran™) and 100 U/mL penicillin and 100 µg/mL streptomycin (Eurobio™).

Nasal and bronchial epithelial cell cultures were established from nasal or bronchial brushings, as previously described[52,53]. Nasal and basal epithelial cells were cultured in PneumaCult™-Ex Plus Medium (StemCell Technologies) supplemented with penicillin-streptomycin-Amphotericin B 1X (100X, Gibco).

All cell types were cultured at 37 °C, 5% CO2 in a humidified chamber.

Construction of eGFP$^+$ cell models

HEK293T cells, K562 cells and hFFs were transduced with a lentivirus containing the gene encoding eGFP (enhanced green fluorescent protein) and a puromycin resistance gene, under the dependence of the ubiquitous strong constitutive promoter MND (myeloproliferative sarcoma virus enhancer, negative control region deleted, dl587rev primer-binding site substituted). This lentivirus was produced and titrated by the Vect'UB vectorology platform at Bordeaux University. HEK293T cells, K562 cells and hFFs were transduced at a multiplicity of infection (MOI) of 0.1, 1 and 2, respectively, to obtain a low copy number of the integrated vector. Transduced cells were selected 96h after transduction by adding puromycin (2 µg/mL for 48h, Gibco) to their culture medium. Hereafter, these cells are referred to as eGFP$^+$-HEK293T cells, eGFP$^+$-K562 cells and eGFP$^+$-hFFs.

RNP transfection and gene-editing tools

The crRNAs were designed using CHOP-CHOP software (chopchop.cbu.uib.no). Then the tracrRNA part (eventually modified for one of the loops and lengthwise) was added to reconstitute the gRNA.

gRNAs and ssODN templates for HDR correction were ordered from Integrated DNA Technologies (Coralville, USA). Their sequences are given in Supplementary Tables 1 and 2.

Eventually, annealing between sgRNA and ssODN template(s) to form sgRNA-template hybrids (ZE1, ZE1a, ZE1b, ZE1L, ZE1La, ZE1Lb, ZEN and ZENmax) or sgRNA-templates hybrid (ZE1D) was performed by mixing the components either in equimolar proportion (1:1) for ZE1, ZE1a, ZE1b, ZE1L, ZE1La, ZE1Lb, ZEN and ZENmax systems, or with a double template (1:2) for the ZE1D. The components were then heated for 5 minutes in a dry bath at 95°C before allowing them to cool at room temperature.

The different components of the CRISPR-Cas9 system (Alt-R® S.p. HiFi Cas9 Nuclease V3 (abbreviated hereafter as Cas9 nuclease) or Alt-R S.p.Cas9 D10A Nickase V3 protein (abbreviated hereafter as Cas9 nickase) both from Integrated DNA Technologies, with either split sgRNA and ssODN template or sgRNA-template(s) hybrid(s) were combined to form an RNP. They were mixed and then incubated for 10-20 minutes at room temperature. For this, 10 µg (for HEK293T cells, K562 cells and hFFs) or 17 µg (for other cells) of nuclease or nickase Cas9 and 3.9 µM (for HEK293T cells, K562 cells and hFFs) or 6.5 µM (for other cells) of sgRNA, ssODN template or sgRNA-template(s) hybrids for ZEs were mixed. Finally, 3.9 µM of Alt-R Cas9 Electroporation Enhancer solution (Integrated DNA Technologies) were added to the RNP complex to improve electroporation efficiency.

Cells were transfected by electroporation using the Nucleofector 4D AMAXA electroporation system (Lonza®, Bale, Switzerland). In brief, 5.10^4 to 3.10^5 depending on the cell type were resuspended in SF Cell Line 4D-Nucleofector® (HEK293T cells or K562 cells) or P3 Primary Cell Line 4D-Nucleofector® (hFFs, $CD34^+$ HSPCs, pulmonary epithelial basal cells, nasal epithelial cells and bronchial epithelial cells) and added to the RNP complex. Then cells were nucleofected using DG-150, FF-120, CZ-167, DO-100 or DC-100 programs, respectively.

Cells were then cultured as described above for 5-15 days depending on the editing analysis method.

Edition analysis

HDR and imprecise editing (InDels) analysis by flow cytometry

For the *eGFP* target, precise editing allows the switch from eGFP to BFP. At least 6 days after editing and before flow cytometry analysis, cells were recovered in a PBS (phosphate buffered saline, Gibco) - EDTA (ethylenediaminetetraacetic acid, 2 mM, Sigma-Aldrich) solution. Cells were analyzed for fluorescence using the BD FACSCanto II analyzer (BD Biosciences, Le Pont de Claix, France) at the cytometry platform at University of Bordeaux (UB'FACSility). Excitation wavelengths of 488 and 405 nm were used to detect eGFP and BFP fluorescence in the FITC (Fluorescein-5-isothiocyanate) (530/30 filter) and Pacific Blue (450/50 filter) channels, respectively. The data presented are from the analysis of at least 10,000 events. The percentages of $eGFP^+/BFP^-$, $eGFP^-/BFP^+$, and $eGFP^-/BFP^-$ correspond to cells unedited, edited by HDR, or with InDels, respectively. The percentages of BFP^+ or $eGFP^-/BFP^-$ cells shown in the graphs were calculated by subtracting the percentages of BFP^+ or $eGFP^-/BFP^-$ cells, respectively, from a sample of cells from the corresponding lineage not transfected with RNP when these were non-zero. Then, the percentage of BFP^+, $eGFP^-/BFP^-$ or $eGFP^+/BFP^-$ cells were normalized to recover a total of 100%.

HDR analysis by RFLP

If a restriction site is added to the ssODN template sequence, the HDR rate can be measured by RFLP (restriction fragment length polymorphism). At least 5 days after editing, genomic DNA was extracted from cell pellets using Nucleospin® Tissue (Macherey-Nagel, Duren, Germany) according to the manufacturer's protocol. The genomic region flanking the edited site was amplified by PCR (HotStarTaq Plus DNA polymerase, Qiagen®, Venlo, Netherlands) with adequate primers (Supplementary Table 3). PCR products were purified with Nucleospin® Gel and PCR Clean-up (Macherey-Nagel) and digested with SacI restriction enzyme (New England Biolabs, Ipswich, USA) for at least 1 h at 37 °C. Then, digestion products were loaded into the Agilent® 2200 TapeStation (Santa Clara, USA) capillary electrophoresis using D1000 ScreenTape and D1000 reagents according to the manufacturer's protocol. Quality control of enzymatic digestion efficiency was included in each assay.

HDR analysis by Nanopore sequencing

At least 5 days after editing, genomic DNA was extracted from cell pellets using Nucleospin® Tissue (Macherey-Nagel) according to the manufacturer's protocol. The genomic region flanking the edited site was amplified by High-Fidelity PCR (Phusion High-Fidelity DNA Polymerase, New England Biolabs) using 35 cycles under recommended manufacturer's protocol with adequate primers (Supplementary Table 3). A sequencing library was prepared using the Rapid Barcoding Kit 96 V14 (SQK-RBK114.96, Oxford Nanopore Technologies, Oxford, UK) according to the manufacturer's protocol. Sequencing was then performed using a MinION Mk1B device and a Flow Cell R10.4.1 (FLO-MIN114) both from Oxford Nanopore Technologies to reach at least 2000 quality-filtered reads per sample (Q score > 8). After sequencing, super-accurate basecalling was performed using MinKNOW (v24.02.6) and FASTQ were aligned on the human reference genome GrCH38 (GCA_0000001405.15) using Epi2Me (v5.1.9) and the wf-alignment pipeline (v1.1.2). Then, BAM were analyzed with two custom bioinformatic scripts in Python (v3.8) using pysam (v0.16). Briefly, one searches specific sequences in the BAM corresponding to unedited, HDR edited sequences or eventually predominant InDels seen with IGV (Integrative Genomics Viewer) visualization to determine the HDR editing rate per read, whereas the other one calculates the proportion of each nucleotide for each selected position to determine the HDR editing rate per base, returning these data in xlsx format (pandas v1.1.3).

Drugs used

Cell cycle synchronization

To evaluate the impact of synchronization on HDR editing efficiency, cells were synchronized in the G0/G1 phase by incubation with palbociclib, also named PF-00080665 or PD 0332991 (1 µM, Sigma Aldrich) 24 h before and 24 h after RNP transfection. To synchronize cells in the S phase, they were incubated with XL413 (20 µM, Selleckchem, Houston, USA) for 24 h before RNP transfection and 24h after RNP transfection.

Cell cycle analyses were performed to check synchronization efficiency in each experiment. Briefly, cells either synchronized or not were harvested, fixed with 4% paraformaldehyde (for 15 minutes)

and permeabilized with Triton 0.5% (Sigma-Aldrich, for 15 minutes). Cells were then incubated overnight with RNAse (100 µg/mL, MoBiTec, Goettingen, Germany) and then for 15 minutes with propidium iodide (4 µg/mL, Biolegend). The samples were examined on a BD Biociences Accuri C6 Plus flow cytometer and the data were analyzed with BD CSampler™ software (BD Biosciences).

HDAC inhibition

To evaluate the impact of HDAC inhibition, cells were incubated 24h before and 48h after edition with either valproic acid (VPA, 0.3, 1 or 3 mM, Sigma-Aldrich), WT-161 (0.5, 2 or 10 nM, MedChemExpress, Monmouth Junction, USA) or sodium butyrate (NaBut, 0.3, 1 or 3 mM, Sigma-Aldrich).

NHEJ inhibition

To modulate the NHEJ pathway, we incubated the cells 24h before and 48h after edition with AZD7648 (1 µM, MedChemExpress).

Nick repair pathway inhibition

To modulate the nick repair pathways, HEK293T and K562 cells were transfected either 48h or 72h before edition with a siRNA targeting *BRCA2* (10 pmol/mL, #s2085 Life Technologies, Carlsbad, USA), respectively. siRNA transfections were performed using Lipofectamine RNAiMAX (Life Technologies) according to the manufacturer's protocol. To determine the efficiency of siRNA knockdown, *BRCA2* mRNA levels were quantified by RT-qPCR relative to control that assayed glyceraldehyde-3-phosphate dehydrogenase (*GAPDH*) transcripts. Briefly, RNA was extracted from cell pellets using Nucleospin® RNA (Macherey-Nagel) according to the manufacturer's protocol. RNA was retro-transcribed into cDNA using high-capacity cDNA reverse transcription (Applied Biosystems, Waltham, USA) according to the manufacturer's protocol. Then qPCR was performed using GoTaq qPCR Master Mix 1X (Promega, Madison, USA) and adequate primers (Supplementary Table 4). Results were analyzed with CFX Maestro 1.0 (BioRad, Hercules, USA)

FAMReD fluorescent cell quantification

At least 15 days after editing, 0.3 mM of 5-aminolevulinic acid hydrochloride (5-ALA, Sigma-Aldrich) was added to hFF medium. After 16h of exposure (overnight), cells were washed twice with PBS and placed in fresh medium. Upon LOH, loss of UROS function can be detected by the appearance of fluorescence due to porphyrin accumulation. Following 8h of clearance, fluorescent cells were quantified by flow cytometry. UV-sensitive porphyrins were excited at 488 nm and the emitted wavelength was approximately 667 nm, detected by the PE-Cy5A PMT channel (FACS Accuri, BD Biosciences). FL-1 is a control green-fluorescent channel used to exclude auto-fluorescent cells.

Statistical analysis and reproducibility

The experimental data presented are from the analysis of several independent experiments. No statistical method was used to predetermine sample size. No data were excluded from the analyses. The experiments were not randomized. Statistical significance was inferred when necessary and formatted using GraphPad Prism 10.3.1 software. To confirm significance, p-values were calculated when analyzing at least three independent experiments. Exact distinct and independent experiments size is indicated in each legend (n). Results are presented as mean ± SD. To compare two groups, the parametric t test (two-sided) or the nonparametric Mann–Whitney test (two-sided) were used when residual distribution was Gaussian/normal or not respectively. If the comparison was done to a condition normalized to 1, the nonparametric Kolmogorov-Smirnov test was used. To compare more than two groups, one-way ANOVA (two-sided) was used and Gaussian/normal residual distribution was checked. To compare several conditions in two groups or more, 2way ANOVA was used and Gaussian/normal residual distribution was checked. If not indicated, the results are not significant. The details (number of independent replicates, statistical test used) are indicated in the legends of the figures.

Reporting summary

Further information on the research design is available in the Nature Portfolio Reporting Summary linked to this article.

References

1. Rouet, P., Smih, F. & Jasin, M. Expression of a site-specific endonuclease stimulates homologous recombination in mammalian cells. *Proc Natl Acad Sci U S A* **91**, 6064–6068 (1994).
2. Bischoff, N., Wimberger, S., Maresca, M. & Brakebusch, C. Improving Precise CRISPR Genome Editing by Small Molecules: Is there a Magic Potion? *Cells* **9**, 1318 (2020).
3. Selvaraj, S. *et al.* High-efficiency transgene integration by homology-directed repair in human primary cells using DNA-PKcs inhibition. *Nat Biotechnol* 1–14 (2023) doi:10.1038/s41587-023-01888-4.
4. Riesenberg, S. *et al.* Efficient high-precision homology-directed repair-dependent genome editing by HDRobust. *Nat Methods* **20**, 1388–1399 (2023).
5. Wimberger, S. *et al.* Simultaneous inhibition of DNA-PK and Polϴ improves integration efficiency and precision of genome editing. *Nat Commun* **14**, 4761 (2023).
6. Schimmel, J. *et al.* Modulating mutational outcomes and improving precise gene editing at CRISPR-Cas9-induced breaks by chemical inhibition of end-joining pathways. *Cell Reports* **42**, (2023).
7. Jin, Y.-Y. *et al.* Enhancing homology-directed repair efficiency with HDR-boosting modular ssDNA donor. *Nat Commun* **15**, 6843 (2024).
8. Rees, H. A., Yeh, W.-H. & Liu, D. R. Development of hRad51–Cas9 nickase fusions that mediate HDR without double-stranded breaks. *Nat Commun* **10**, 2212 (2019).
9. Park, S.-J., Park, S. J., Kwon, Y. W. & Choi, E.-H. Synergistic combination of RAD51-SCR7 improves CRISPR-Cas9 genome editing efficiency by preventing R-loop accumulation. *Molecular Therapy - Nucleic Acids* **35**, 102274 (2024).

10. Charpentier, M. *et al.* CtIP fusion to Cas9 enhances transgene integration by homology-dependent repair. *Nat Commun* **9**, 1133 (2018).
11. Ma, L. *et al.* MiCas9 increases large size gene knock-in rates and reduces undesirable on-target and off-target indel edits. *Nat Commun* **11**, 6082 (2020).
12. Jayavaradhan, R. *et al.* CRISPR-Cas9 fusion to dominant-negative 53BP1 enhances HDR and inhibits NHEJ specifically at Cas9 target sites. *Nat Commun* **10**, 2866 (2019).
13. Carusillo, A. *et al.* A novel Cas9 fusion protein promotes targeted genome editing with reduced mutational burden in primary human cells. *Nucleic Acids Research* **51**, 4660–4673 (2023).
14. Lin, S., Staahl, B. T., Alla, R. K. & Doudna, J. A. Enhanced homology-directed human genome engineering by controlled timing of CRISPR/Cas9 delivery. *Elife* **3**, e04766 (2014).
15. Komor, A. C., Kim, Y. B., Packer, M. S., Zuris, J. A. & Liu, D. R. Programmable editing of a target base in genomic DNA without double-stranded DNA cleavage. *Nature* **533**, 420–424 (2016).
16. Anzalone, A. V. *et al.* Search-and-replace genome editing without double-strand breaks or donor DNA. *Nature* **576**, 149–157 (2019).
17. Ferreira da Silva, J. *et al.* Click editing enables programmable genome writing using DNA polymerases and HUH endonucleases. *Nat Biotechnol* 1–13 (2024) doi:10.1038/s41587-024-02324-x.
18. Wang, J., Sadeghi, C. A. & Frock, R. L. DNA-PKcs suppresses illegitimate chromosome rearrangements. *Nucleic Acids Res* **52**, 5048–5066 (2024).
19. Cullot, G. *et al.* CRISPR-Cas9 genome editing induces megabase-scale chromosomal truncations. *Nat Commun* **10**, (2019).
20. Lee, K. *et al.* Synthetically modified guide RNA and donor DNA are a versatile platform for CRISPR-Cas9 engineering. *eLife* e25312 (2017) doi:10.7554/eLife.25312.
21. Glaser, A., McColl, B. & Vadolas, J. GFP to BFP Conversion: A Versatile Assay for the Quantification of CRISPR/Cas9-mediated Genome Editing. *Mol Ther Nucleic Acids* **5**, (2016).

22. Heim, R., Prasher, D. C. & Tsien, R. Y. Wavelength mutations and posttranslational autoxidation of green fluorescent protein. *Proc Natl Acad Sci U S A* **91**, 12501–12504 (1994).

23. Riesenberg, S., Helmbrecht, N., Kanis, P., Maricic, T. & Pääbo, S. Improved gRNA secondary structures allow editing of target sites resistant to CRISPR-Cas9 cleavage. *Nat Commun* **13**, (2022).

24. Cullot, G. *et al.* Genome editing with the HDR-enhancing DNA-PKcs inhibitor AZD7648 causes large-scale genomic alterations. *Nat Biotechnol* 1–5 (2024) doi:10.1038/s41587-024-02488-6.

25. Fang, X., Yeh, J.-T. & Hwang, T.-C. Pharmacological Responses of the G542X-CFTR to CFTR Modulators. *Front Mol Biosci* **9**, 921680 (2022).

26. Javidi-Parsijani, P. *et al.* CRISPR/Cas9 increases mitotic gene conversion in human cells. *Gene Ther* **27**, 281–296 (2020).

27. Mianné, J. *et al.* CRISPR/Cas9-mediated gene knockout and interallelic gene conversion in human induced pluripotent stem cells using non-integrative bacteriophage-chimeric retrovirus-like particles. *BMC Biol* **20**, 8 (2022).

28. Boutin, J. *et al.* ON-Target Adverse Events of CRISPR-Cas9 Nuclease: More Chaotic than Expected. *CRISPR J* **5**, 19–30 (2022).

29. Cullot, G. *et al.* Cell cycle arrest and p53 prevent ON-target megabase-scale rearrangements induced by CRISPR-Cas9. *Nat Commun* **14**, 4072 (2023).

30. Gopalappa, R., Suresh, B., Ramakrishna, S. & Kim, H. (Henry). Paired D10A Cas9 nickases are sometimes more efficient than individual nucleases for gene disruption. *Nucleic Acids Res* **46**, e71 (2018).

31. Lee, J. *et al.* Prime editing with genuine Cas9 nickases minimizes unwanted indels. *Nat Commun* **14**, 1786 (2023).

32. Vriend, L. E. M. & Krawczyk, P. M. Nick-initiated homologous recombination: Protecting the genome, one strand at a time. *DNA Repair (Amst)* **50**, 1–13 (2017).

33. Davis, L. & Maizels, N. Homology-directed repair of DNA nicks via pathways distinct from canonical double-strand break repair. *Proceedings of the National Academy of Sciences* **111**, E924–E932 (2014).

34. Zhang, Y., Davis, L. & Maizels, N. Pathways and signatures of mutagenesis at targeted DNA nicks. *PLoS Genet* **17**, e1009329 (2021).

35. Liu, B. *et al.* Targeted genome editing with a DNA-dependent DNA polymerase and exogenous DNA-containing templates. *Nat Biotechnol* **42**, 1039–1045 (2024).

36. Savic, N. *et al.* Covalent linkage of the DNA repair template to the CRISPR-Cas9 nuclease enhances homology-directed repair. *eLife* **7**, e33761 (2018).

37. Aird, E. J., Lovendahl, K. N., St. Martin, A., Harris, R. S. & Gordon, W. R. Increasing Cas9-mediated homology-directed repair efficiency through covalent tethering of DNA repair template. *Commun Biol* **1**, 1–6 (2018).

38. Ling, X. *et al.* Improving the efficiency of precise genome editing with site-specific Cas9-oligonucleotide conjugates. *Sci. Adv* **6**, eaaz0051 (2020).

39. Carlson-Stevermer, J. *et al.* Assembly of CRISPR ribonucleoproteins with biotinylated oligonucleotides via an RNA aptamer for precise gene editing. *Nat Commun* **8**, (2017).

40. Simone, B. W. *et al.* Chimeric RNA: DNA TracrRNA Improves Homology-Directed Repair In Vitro and In Vivo. *CRISPR J* **5**, 40–52 (2022).

41. Brault, J. *et al.* CRISPR-Cas9-AAV versus lentivector transduction for genome modification of X-linked severe combined immunodeficiency hematopoietic stem cells. *Front Immunol* **13**, 1067417 (2023).

42. Chen, X. *et al.* In trans paired nicking triggers seamless genome editing without double-stranded DNA cutting. *Nat Commun* **8**, 657 (2017).

43. Davis, L. & Maizels, N. DNA Nicks Promote Efficient and Safe Targeted Gene Correction. *PLoS One* **6**, e23981 (2011).

44. Satomura, A. *et al.* Precise genome-wide base editing by the CRISPR Nickase system in yeast. *Sci Rep* **7**, 2095 (2017).

45. Coelho, M. A. *et al.* Base editing screens map mutations affecting interferon-γ signaling in cancer. *Cancer Cell* **41**, 288-303.e6 (2023).

46. Chen, P. J. *et al.* Enhanced prime editing systems by manipulating cellular determinants of editing outcomes. *Cell* **184**, 5635-5652.e29 (2021).

47. Ferreira da Silva, J. *et al.* Prime editing efficiency and fidelity are enhanced in the absence of mismatch repair. *Nat Commun* **13**, (2022).

48. Fiumara, M. *et al.* Genotoxic effects of base and prime editing in human hematopoietic stem cells. *Nat Biotechnol* 1–15 (2023) doi:10.1038/s41587-023-01915-4.

49. Lim, P. X., Zaman, M., Feng, W. & Jasin, M. BRCA2 promotes genomic integrity and therapy resistance primarily through its role in homology-directed repair. *Mol Cell* **84**, 447-462.e10 (2024).

50. Björnson, Y. *et al.* The effect of histone deacetylase inhibitors on the efficiency of the CRISPR/Cas9 system. *Biochem Biophys Rep* **35**, 101513 (2023).

51. Liu, N. *et al.* HDAC inhibitors improve CRISPR-Cas9 mediated prime editing and base editing. *Mol Ther Nucleic Acids* **29**, 36–46 (2022).

52. Trian, T. *et al.* House Dust Mites Induce Proliferation of Severe Asthmatic Smooth Muscle Cells via an Epithelium-Dependent Pathway. *Am J Respir Crit Care Med* **191**, 538–546 (2015).

53. Esteves, P. *et al.* Asthmatic bronchial smooth muscle increases rhinovirus replication within the bronchial epithelium. *Cell Reports* **38**, (2022).

Acknowledgements

We thank all the staff from Vect'UB, FACSility and One cell facilities at University of Bordeaux (TBMCore), Sandrine Hamon, Stephanie Lannelongue and all the BRIC administrative staff for administrative assistance and financial management, Bagatelle Hospital (Talence, France) for cord

blood samples and Ray Cooke for copyediting the manuscript. C.T. is supported by funding from the AFM-Telethon (#24581). This work was supported by an AFM-Telethon grant (#24136), CoPOC ZIP-CRISPR (RVF23035GSA) and the French ANR grants GENOTOX (ANR-21-CE18-0002-01) and CRISPR SAFE (ANR-PRME-24-CE52).

Author contributions

C.T., J.R. , F.M.G. and A.B: design and analysis of data; C.T. , F.M.G. and A.B: drafting of manuscript; A.B., F.M.G.: supervision, funding acquisition, final approval of manuscript; C.T., J.R., M.R., V.M., S.F, R.E.: performing editing experiments and associated analysis; V.M., C.T.: Nanopore sequencing bioinformatic analysis; C.T., I.L.G, C.B.: performing cell cycle analysis; I.L.G: isolation of HSPCs; T.T., S.B.: obtention of pulmonary epithelial basal cells, nasal epithelial cells and bronchial epithelial cells; J.B.: helpful discussion in the field of CRISPR-Cas9; S.D., J.B.: proofreading of manuscript.

Competing interests

C.T, J.R., A.B., and F.M.G declared a patent application EP25305256 filed on February 26, 2025 and claims the use of ZIP editing to increase HDR editing efficiency with CRISPR. The remaining authors declare no competing interests.

FIGURE LEGENDS

Fig. 1: Set up of Zip Editors (ZE) to increase HDR editing efficiency with Cas9 nuclease in cell lines. **a** Representation of RNPs “UNZIP" (Cas9 nuclease with free ssODN template) and “Zip Editing (ZE) 1” (Cas9 nuclease with ssODN template import: elongated ssODN - in light green - for hybridization to the elongated gRNA - in light pink-). **b** Editing strategy to convert eGFP into BFP. T65S and Y66H amino acid substitutions correspond to a shift in the fluorescence excitation and emission spectra of the protein, converting eGFP to BFP. **c** Construction of cell models and result analysis timeline. **d** Illustrative cytometry results of eGFP^{+}-HEK293T cells, unedited, edited by UNZIP or edited by ZE1**. e**

and f Flow cytometry quantification of the edition with Cas9 nuclease with (ZE1) or without (UNZIP) the correction template physically bound to the gRNA in eGFP$^+$-HEK293T cells (n=4) and eGFP$^+$-K562 cells (n=8), respectively. The proportions of cells expressing BFP (HDR-edited), eGFP (unedited) or neither of these fluorophores (imprecisely edited, with InDels) one week after transfection are reported. The mean ± SD is shown. The HDR/InDels ratio is indicated at the top of the graphs. Statistical significance determined by two-way ANOVA. Schemas created with BioRender.com.

Fig. 2: Improvement of ZE to boost HDR editing with Cas9 nuclease in cell lines and primary cells. a Representation of RNPs used in the ZE1D and ZE1L=ZEmax import systems. **b** Flow cytometry quantification of the HDR edition with Cas9 nuclease with ZE1D (n=4) and ZE1L (n=6) in eGFP$^+$-K562 cells. The proportions of cells expressing BFP one week after transfection are reported. Fold-changes indicate the fold-increase between the ZE1D or ZE1L systems relative to ZE1. The mean ± SD is shown. Statistical significance to ZE1 determined by Kolmogorov-Smirnov test. **c** Editing strategy to edit *HBB* in HEK293T cells. **d** Representation of UNZIP2 system. **e** Nanopore sequencing to quantify HDR editing per base with UNZIP2 or ZEmax (n=3). The mean ± SD is shown. Statistical significance determined by two-way ANOVA. **f** Flow cytometry quantification of the edition with Cas9 nuclease with ZEmax or UNZIP in eGFP$^+$-hFFs (n=5). The proportions of cells expressing BFP, eGFP or neither of these fluorophores one week after transfection are reported. The mean ± SD is shown. The HDR/InDels ratio is indicated at the top of the graphs. Statistical significance is determined by two-way ANOVA. **g** Flow cytometry quantification of the HDR edition with Cas9 nuclease with UNZIP or ZEmax and with or without inhibition of NHEJ repair with AZD7648 in eGFP$^+$-hFFs (n=4). The proportions of cells expressing BFP one week after transfection are reported. The mean ± SD is shown. The HDR/InDels ratio is indicated at the top of the graphs. Statistical significance determined by one-way ANOVA. **h** Editing strategy to edit *UROS* in CD34$^+$ cells. **i** Capillary electrophoresis of *SacI* digestion products to quantify HDR editing with UNZIP2 or ZEmax (n=4). The mean ± SD is shown. Statistical significance determined by unpaired t-test. Schemas created with BioRender.com.

Fig. 3: Validation of ZEmax technology for *CFTR* editing in pulmonary basal, bronchial and nasal epithelial cells. Obtention of human healthy pulmonary epithelial basal cells and editing strategy to model *CFTR* G542X mutation and insert *SacI* restriction site. **b** Capillary electrophoresis of *SacI* digestion products to quantify HDR editing with UNZIP or ZEmax (n=4). The mean ± SD is shown. Statistical significance determined by paired t-test. **c** Obtention of human nasal and bronchial epithelial cells from a patient with cystic fibrosis carrying the *CFTR* G542X rare mutation and editing strategy i) to correct *CFTR* G542X mutation and ii) to add other silent modifications to prevent re-cut by nuclease Cas9. **d** Nanopore sequencing to quantify HDR editing per read (total HDR, 7 modifications) with UNZIP2 or ZEmax in nasal (left panel) or bronchial (right panel) epithelial cells (n=3). The mean ± SD is shown. Statistical significance compared to unedited cells determined by one-way ANOVA. **e** Nanopore sequencing to quantify HDR editing per base with UNZIP2 or ZEmax in nasal (left panel) or bronchial (right panel) epithelial cells (n=3). The mean ± SD is shown. Schemas created with BioRender.com.

Fig 4: Increased availability of HDR template with ZEN is essential to repair nicks by HDR. a Representation of RNPs "UNZEN" (Cas9 nickase with free ssODN template) and "Zip Editing Nickase" (ZEN, Cas9 nickase with ssODN import using hybridization of 5'-elongated ssODN to the t-lock gRNA). **b** Flow cytometry quantification of the edition with Cas9 nickase with (ZEN) or without (UNZEN) the correction template physically bound to the gRNA in eGFP$^+$-HEK293T cells (n=10), eGFP$^+$-K562 cells (n=8), and eGFP$^+$-hFFs (n=4). The proportions of cells expressing BFP (HDR-edited) one week after transfection are reported. The mean ± SD is shown. Statistical significance determined by unpaired t-test (eGFP$^+$-HEK293T cells, eGFP$^+$-hFFs) or Mann-Whitney test (eGFP$^+$-K562 cells). **c** Editing strategy to edit *UROS* in hFFs. **d** Representation of "UNZEN2" (control of ZEN with modified gRNA but without ssODN-gRNA annealing). **e** Nanopore sequencing to quantify HDR editing per read (total HDR, 3 modifications) with UNZEN2 or ZEN (n=4). The mean ± SD is shown. Statistical significance determined by unpaired t-test. **f** Nanopore sequencing to quantify HDR editing per base with UNZEN2

or ZEN (n=4). The mean ± SD is shown. Statistical significance determined by two-way ANOVA. Schemas created with BioRender.com.

Fig. 5: Iterative editing and ssODN template design improve HDR editing with ZEN. a Timeline for iterative transfections (RNPs nucleofection). **b** Flow cytometry quantification of edition after 1, 2 or 3 transfection(s) with ZEN in eGFP$^+$-hFFs (n=3). The proportions of cells expressing BFP (HDR-edited) one week after transfection are reported. The mean ± SD is shown. Statistical significance determined by one-way ANOVA. **c** Nanopore sequencing quantification of edition after 1, 2 or 3 transfection(s) with ZEN in hFFs (n=4). Total HDR (3 modifications) rates per read are reported. The mean ± SD is shown. Statistical significance determined by one-way ANOVA. **d** Representation of BFP-ssODN template position relative to the cut site used for ZEN or ZENmax. **e** Flow cytometry quantification of edition with ZEN or ZENmax in eGFP$^+$-hFFs (n=8). The proportions of cells expressing BFP (HDR-edited) one week after transfection are reported. The mean ± SD is shown. Statistical significance determined by unpaired t-test. **f** Flow cytometry quantification of edition after 1, 2 or 3 transfection(s) with ZENmax in eGFP$^+$-hFFs (n=3). The proportions of cells expressing BFP (HDR-edited) one week after transfection are reported. The mean ± SD is shown. Statistical significance determined by one-way ANOVA.

Fig. 6: Modulation of 'cell state' can be associated with ZEN to increase HDR editing. a Illustrative cell cycle results of eGFP$^+$-hFFs with palbociclib, XL413 (right panel) or without drug (left panel). Flow cytometry quantification of the proportion of eGFP$^+$-hFFs in G0/G1 or S/G2/M phases with palbociclib, XL413 or without drug (right panel, n=4). The mean ± SD is shown. Statistical significance to cells without drugs determined by two-way ANOVA. **b** Timeline for transfections (RNPs nucleofection) in presence of drugs. **c** Flow cytometry quantification of HDR edition with Cas9 nickase (ZENmax) with or without synchronization of eGFP$^+$-hFFs in G0/G1 phase with palbociclib or in S/G2/M phases with XL413 (n=4). The proportions of cells expressing BFP (HDR-edited) one week after transfection are reported. Fold changes indicate fold increases between conditions with or without drug. The mean ± SD is shown. Statistical significance to ZENmax without drugs determined

by Kolmogorov-Smirnov test. **d** Flow cytometry quantification of HDR edition with nickase Cas9 (ZEN) with or without VPA (n=3), WT-161 (n=3) or NaBut (n=5) exposure. The proportion of cells expressing BFP (HDR-edited) one week after transfection is reported. Fold changes indicate fold increases between the conditions with either VPA, WT-161 or NaBut and the condition without drug. The mean ± SD is shown. Statistical significance determined by Kruskal-Wallis test. **d** Nanopore sequencing to quantify *UROS* HDR editing per read with Cas9 nickase (ZEN) with or without NaBut in hFFs (n=4). Fold changes indicate fold increases between the conditions with or without NaBut. The mean ± SD is shown. Statistical significance determined by Kolmogorov-Smirnov test. Schemas created with BioRender.com.

Supplementary Fig. 1: Zip Editing development. a Representation of RNPs used in the ZE1a (ZE1 with 3-'elongated ssODN template) and ZE1b (ZE1 with additive t-lock loop in the gRNA) import systems. **b** Flow cytometry quantification of HDR edition with Cas9 nuclease with ZE1a or ZE1b in eGFP^{+}-K562 cells (n=4). The proportions of cells expressing BFP (HDR-edited) one week after transfection are reported. Fold changes indicate fold increases between ZE1a or ZE1b relative to ZE1. The mean ± SD is shown. **c** Representation of RNPs used in the ZE1La (ZE1L with 3-'over-elongated ssODN template) and ZE1Lb (ZE1L with ssODN 3'-hybridization to the gRNA, instead of 5') import systems. **d** Flow cytometry quantification of HDR edition with Cas9 nuclease with ZE1La (n=4) and ZE1Lb (n=3) in eGFP^{+}-K562 cells. The proportions of cells expressing BFP (HDR-edited) one week after transfection are reported. Fold changes indicate fold increases between ZE1La or ZE1Lb relative to ZE1L. The mean ± SD is shown. Statistical significance to ZE1L determined by Kolmogorov-Smirnov test. Schemas created with BioRender.com.

Supplementary Fig. 2: FAMReD technology to detect loss of heterozygosity (LOH) after CRISPR editing. a FAMReD system to detect and quantify LOH after CRISPR editing and editing strategy to edit *SORCS1* (insertion of *SacI* restriction site) in hFFs. **b** Capillary electrophoresis of *SacI* digestion products to quantify HDR editing with UNZIP2 or ZEmax (n=4). The mean ± SD is shown. **c** LOH quantification after CRISPR editing with sgRNA only, UNZIP2 or ZEmax (n=4). The mean ± SD is shown.

Supplementary Fig. 3: Modulation of DNA repair pathways can be associated with ZEN to increase HDR editing. a RTqPCR quantification of *BRCA2* mRNA expression levels over time after transfection of siRNA directed against *BRCA2* in HEK293T cells (left panel, n=2) or K562 cells (right panel, n=2). Values are normalized to *GAPDH* expression levels. The mean is shown. **b** Flow cytometry quantification of HDR edition with Cas9 nickase (ZEN) with or without inhibition of *BRCA2* by siRNA during edition in eGFP$^+$-HEK293T cells (left panel, n=3) or eGFP$^+$-K562 cells (right panel, n=4). The proportions of cells expressing BFP (HDR-edited) one week after transfection are reported. The mean ± SD is shown. Statistical significance determined by unpaired t-test. **c** Flow cytometry quantification of imprecise edition with Cas9 nickase (ZEN) with or without inhibition of *BRCA2* by siRNA in eGFP$^+$-HEK293T cells (left panel, n=3) or eGFP$^+$-K562 cells (right panel, n=4). The proportions of cells expressing neither BFP nor eGFP one week after transfection are reported. The mean ± SD is shown. Statistical significance determined by one-way ANOVA.

Supplementary Table 1: gRNA sequences for CRISPR-Cas9 editing.

Supplementary Table 2: HDR ssODN template sequences for CRISPR-Cas9 HDR editing.

Supplementary Table 3: PCR primer sequences.

Supplementary Table 4: RTqPCR primer sequences.

Fig. 1

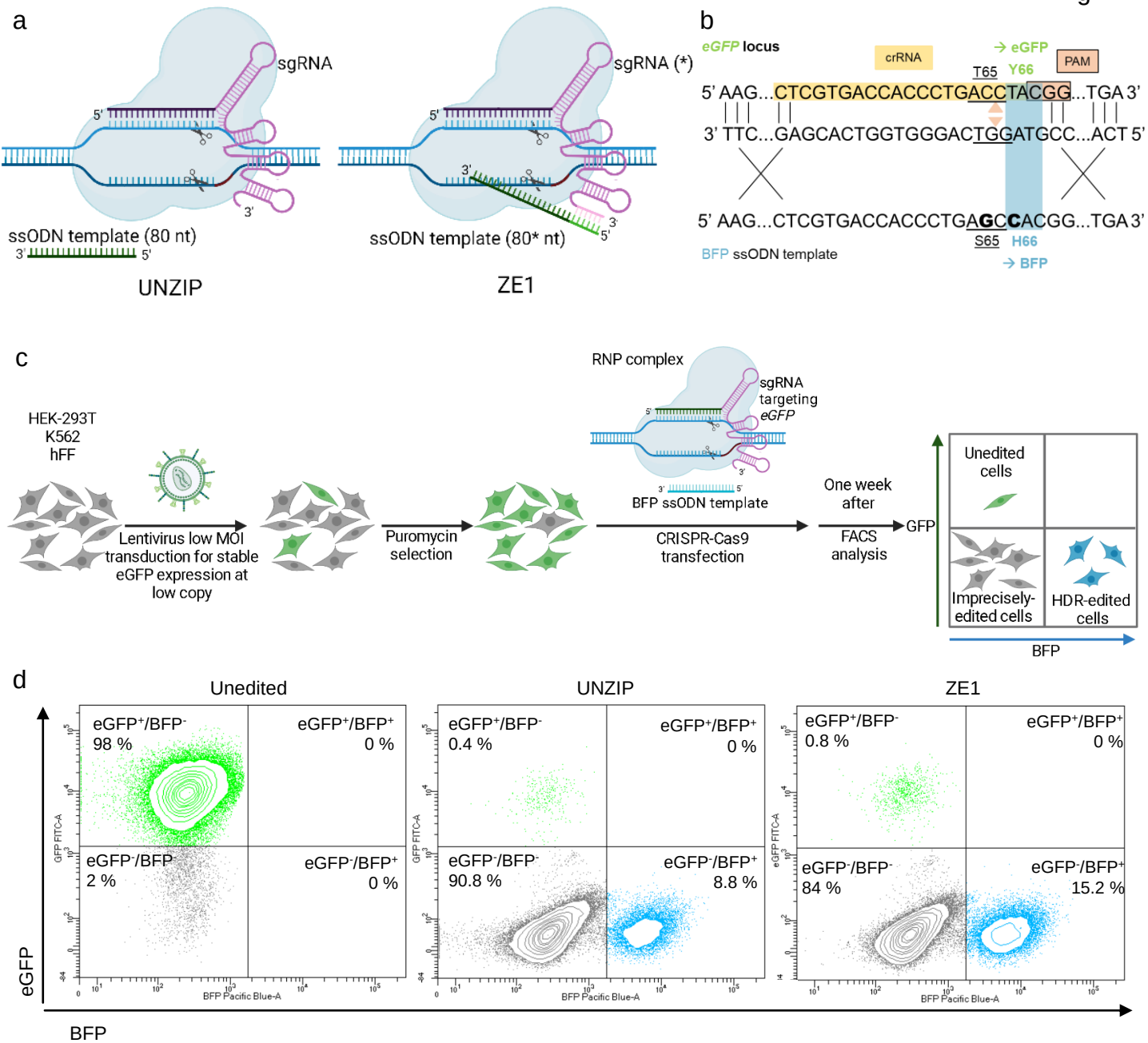
a
sgRNA
5'
3'
ssODN template (80 nt)
3' 5'
UNZIP
sgRNA (*)
ssODN template (80* nt)
ZE1
b
eGFP locus
crRNA
→ eGFP
PAM
T65 Y66
5' AAG...CTCGTGACCACCCTGACCTACGG...TGA 3'
3' TTC...GAGCACTGGTGGGACTGGATGCC...ACT 5'
5' AAG...CTCGTGACCACCCTGAGCCACGG...TGA 3'
S65 H66
BFP ssODN template
→ BFP
c
HEK-293T
K562
hFF
Lentivirus low MOI transduction for stable eGFP expression at low copy
Puromycin selection
RNP complex
sgRNA targeting eGFP
BFP ssODN template
CRISPR-Cas9 transfection
One week after
FACS analysis
GFP
Unedited cells
Imprecisely-edited cells
HDR-edited cells
BFP
d
Unedited
UNZIP
ZE1
eGFP+/BFP-
98 %
eGFP+/BFP+
0 %
eGFP-/BFP-
2 %
eGFP-/BFP+
0 %
0.4 %
90.8 %
8.8 %
0.8 %
84 %
15.2 %
GFP FITC-A
BFP Pacific Blue-A
eGFP
BFP
e
eGFP+-HEK293T
HDR/InDels
0.09
0.18
<0.0001
Percentage of cells (%)
eGFP+/BFP-cells - unedited
eGFP-/BFP- cells - InDels
BFP+cells - HDR
UNZIP
ZE1
f
eGFP+-K562
0.06
0.12
0.0025
0.0042

Fig. 1: Set up of Zip Editors (ZE) to increase HDR editing efficiency with nuclease Cas9 in cell lines. **a** Representation of RNPs “UNZIP" (nuclease Cas9 with free ssODN template) and “Zip Editing (ZE) 1” (nuclease Cas9 with ssODN template import: elongated ssODN - in light green - for hybridization to the elongated gRNA - in light pink-). **b** Editing strategy to convert eGFP into BFP. T65S and Y66H amino acid substitutions correspond to a shift in the fluorescence excitation and emission spectra of the protein, converting eGFP to BFP. **c** Construction of cell models and result analysis timeline. **d** Illustrative cytometry results of $eGFP^+$-HEK293T cells, unedited, edited by UNZIP or edited by ZE1**. e and f** Flow cytometry quantification of the edition with nuclease Cas9 with (ZE1) or without (UNZIP) the correction template physically bound to the gRNA in $eGFP^+$-HEK293T cells (n=4) and $eGFP^+$-K562 cells (n=8), respectively. The proportions of cells expressing BFP (HDR-edited), eGFP (unedited) or neither of these fluorophores (imprecisely edited, with InDels) one week after transfection are reported. The mean ± SD is shown. The HDR/InDels ratio is indicated at the top of the graphs. Statistical significance determined by two-way ANOVA. Schemas created with BioRender.com.

Fig. 2

a

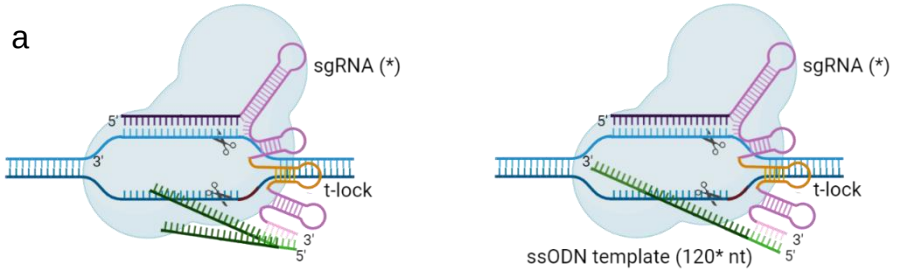

ZE1D
(ZE1 + t-lock loop
+ double ssODN template import)

ZE1L = ZEmax
(ZE1 + t-lock loop
+ 3' elongated ssODN template)

b

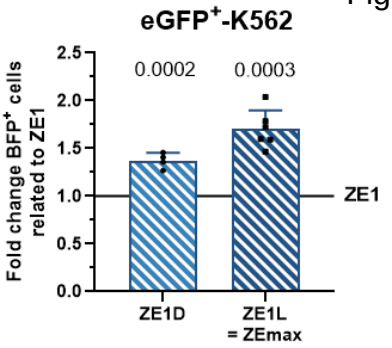

c

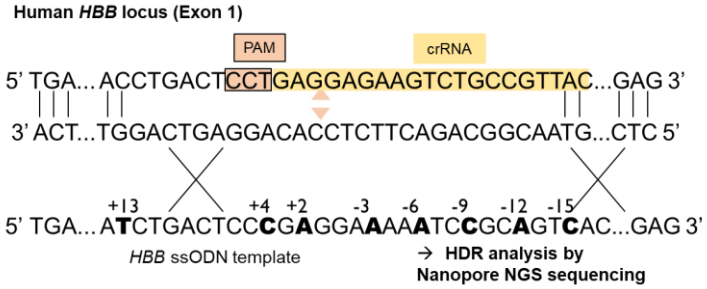

d

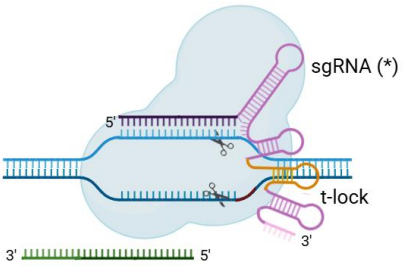

UNZIP2
(UNZIP + t-lock loop
+ 3' elongated ssODN template)

e

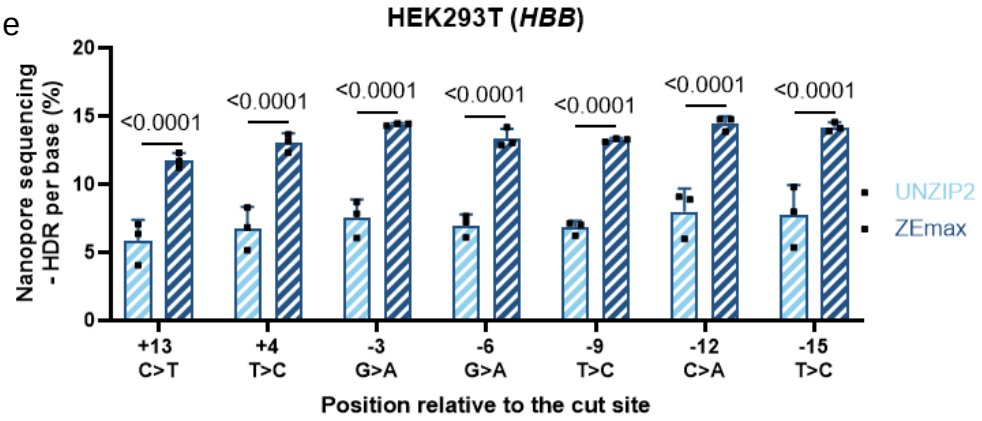

f

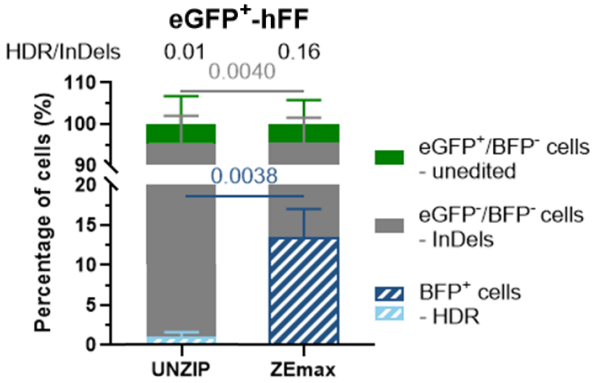

g

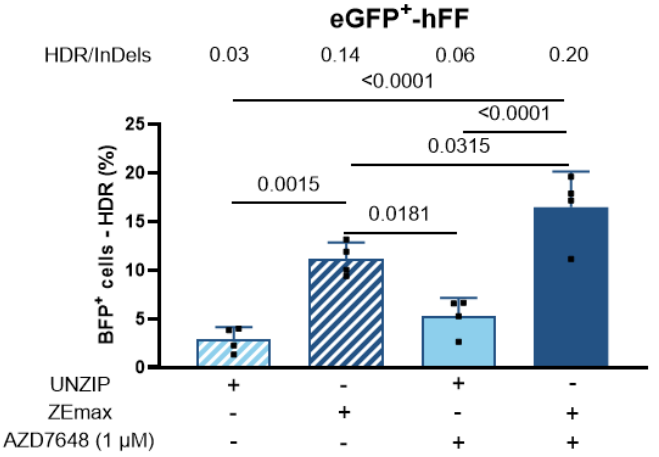

h

Human primary cells:
cord blood CD34+ cells

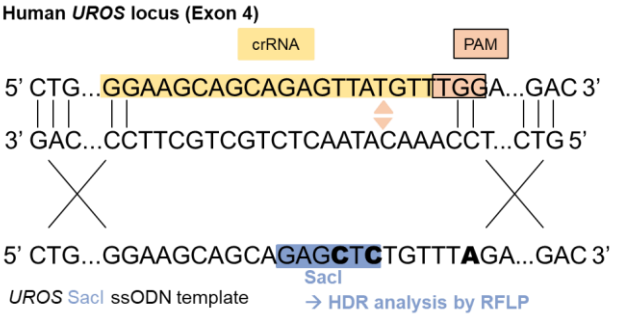

i

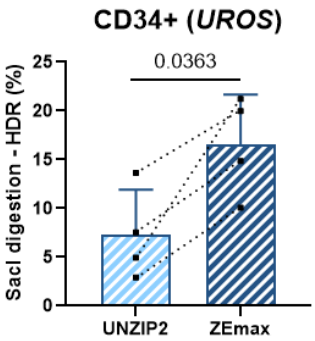

Fig. 2: Improvement of ZE to boost HDR editing with nuclease Cas9 in cell lines and primary cells. a Representation of RNPs used in the ZE1D and ZE1L=ZEmax import systems. **b** Flow cytometry quantification of the HDR edition with nuclease Cas9 with ZE1D (n=4) and ZE1L (n=6) in eGFP^{+}-K562 cells. The proportions of cells expressing BFP one week after transfection are reported. Fold-changes indicate the fold-increase between the ZE1D or ZE1L systems relative to ZE1. The mean ± SD is shown. Statistical significance to ZE1 determined by Kolmogorov-Smirnov test. **c** Editing strategy to edit *HBB* in HEK293T cells. **d** Representation of UNZIP2 system. **e** Nanopore sequencing to quantify HDR editing per base with UNZIP2 or ZEmax (n=3). The mean ± SD is shown. Statistical significance determined by two-way ANOVA. **f** Flow cytometry quantification of the edition with nuclease Cas9 with ZEmax or UNZIP in eGFP^{+}-hFFs (n=5). The proportions of cells expressing BFP, eGFP or neither of these fluorophores one week after transfection are reported. The mean ± SD is shown. The HDR/InDels ratio is indicated at the top of the graphs. Statistical significance determined by two-way ANOVA. **g** Flow cytometry quantification of the HDR edition with nuclease Cas9 with UNZIP or ZEmax and with or without inhibition of NHEJ repair with AZD7648 in eGFP^{+}-hFFs (n=4). The proportions of cells expressing BFP one week after transfection are reported. The mean ± SD is shown. The HDR/InDels ratio is indicated at the top of the graphs. Statistical significance determined by one-way ANOVA. **h** Editing strategy to edit *UROS* in CD34^{+} cells. **i** Capillary electrophoresis of *SacI* digestion products to quantify HDR editing with UNZIP2 or ZEmax (n=4). The mean ± SD is shown. Statistical significance determined by unpaired t-test. Schemas created with BioRender.com.

Fig. 3

a

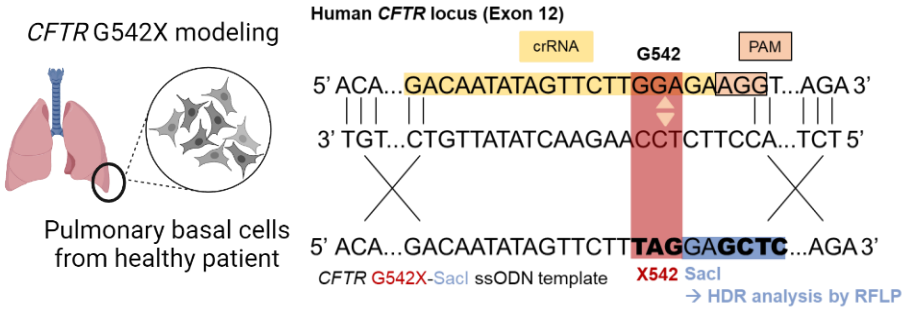
CFTR G542X modeling
Pulmonary basal cells from healthy patient
Human CFTR locus (Exon 12)
crRNA
G542
PAM
5' ACA...GACAATATAGTTCTTGGAGAAGGT...AGA 3'
3' TGT...CTGTTATATCAAGAACCTCTTCCA...TCT 5'
5' ACA...GACAATATAGTTCTTTAGGAGCTC...AGA 3'
CFTR G542X-SacI ssODN template
X542 SacI
→ HDR analysis by RFLP

b

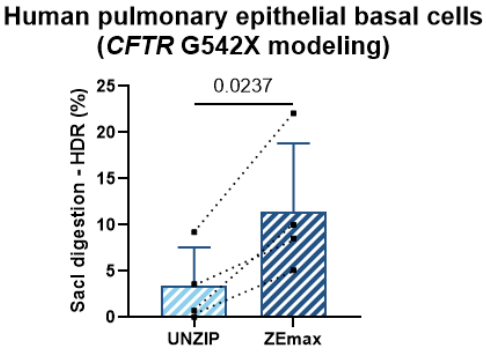
Human pulmonary epithelial basal cells (CFTR G542X modeling)
0.0237
SacI digestion - HDR (%)
25
20
15
10
5
0
UNZIP
ZEmax

c

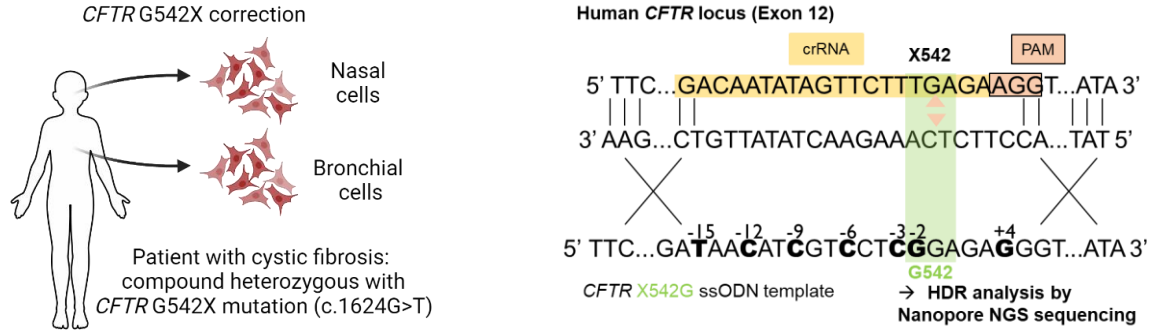
CFTR G542X correction
Nasal cells
Bronchial cells
Patient with cystic fibrosis: compound heterozygous with CFTR G542X mutation (c.1624G>T)
Human CFTR locus (Exon 12)
crRNA
X542
PAM
5' TTC...GACAATATAGTTCTTTGAGAAGGT...ATA 3'
3' AAG...CTGTTATATCAAGAAACTCTTCCA...TAT 5'
-15 -12 -9 -6 -3 -2 +4
5' TTC...GATAACATCGTCCTCGGAGAGGGT...ATA 3'
G542
CFTR X542G ssODN template
→ HDR analysis by Nanopore NGS sequencing

d

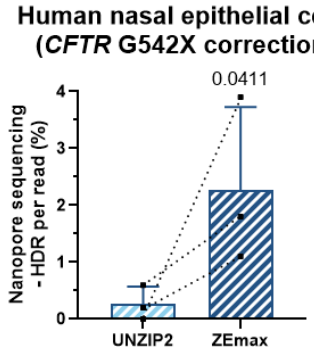
Human nasal epithelial cells (CFTR G542X correction)
0.0411
Nanopore sequencing - HDR per read (%)
4
3
2
1
0
UNZIP2
ZEmax

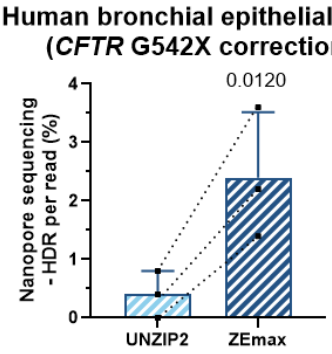
Human bronchial epithelial cells (CFTR G542X correction)
0.0120
Nanopore sequencing - HDR per read (%)
4
3
2
1
0
UNZIP2
ZEmax

e

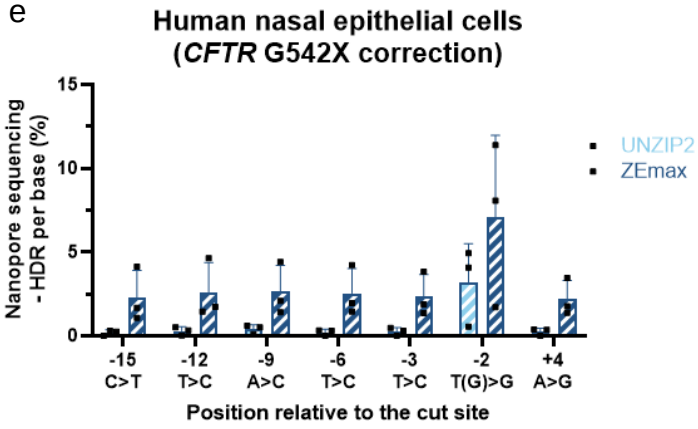
Human nasal epithelial cells (CFTR G542X correction)
Nanopore sequencing - HDR per base (%)
15
10
5
0
UNZIP2
ZEmax
-15 C>T
-12 T>C
-9 A>C
-6 T>C
-3 T>C
-2 T(G)>G
+4 A>G
Position relative to the cut site

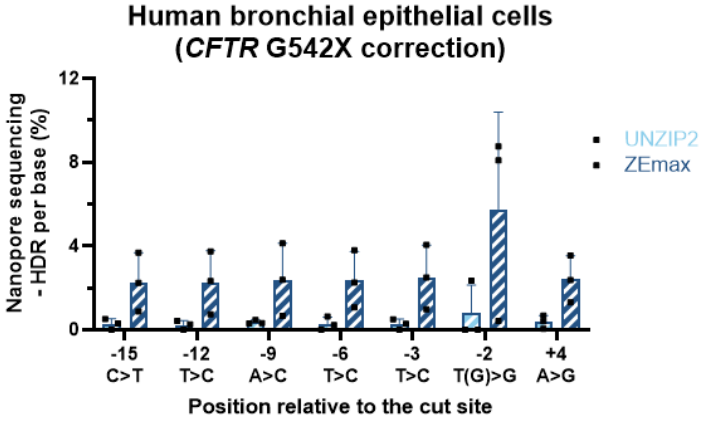
Human bronchial epithelial cells (CFTR G542X correction)
Nanopore sequencing - HDR per base (%)
12
8
4
0
UNZIP2
ZEmax
-15 C>T
-12 T>C
-9 A>C
-6 T>C
-3 T>C
-2 T(G)>G
+4 A>G
Position relative to the cut site

Fig. 3: Validation of ZEmax technology for *CFTR* editing in pulmonary basal, bronchial and nasal epithelial cells. Obtention of human healthy pulmonary epithelial basal cells and editing strategy to model *CFTR* G542X mutation and insert *SacI* restriction site. **b** Capillary electrophoresis of *SacI* digestion products to quantify HDR editing with UNZIP or ZEmax (n=4). The mean ± SD is shown. Statistical significance determined by paired t-test. **c** Obtention of human nasal and bronchial epithelial cells from a patient with cystic fibrosis carrying the *CFTR* G542X rare mutation and editing strategy i) to correct *CFTR* G542X mutation and ii) to add other silent modifications to prevent re-cut by nuclease Cas9. **d** Nanopore sequencing to quantify HDR editing per read (total HDR, 7 modifications) with UNZIP2 or ZEmax in nasal (left panel) or bronchial (right panel) epithelial cells (n=3). The mean ± SD is shown. Statistical significance compared to unedited cells determined by one-way ANOVA. **e** Nanopore sequencing to quantify HDR editing per base with UNZIP2 or ZEmax in nasal (left panel) or bronchial (right panel) epithelial cells (n=3). The mean ± SD is shown. Schemas created with BioRender.com.

Fig. 4

a

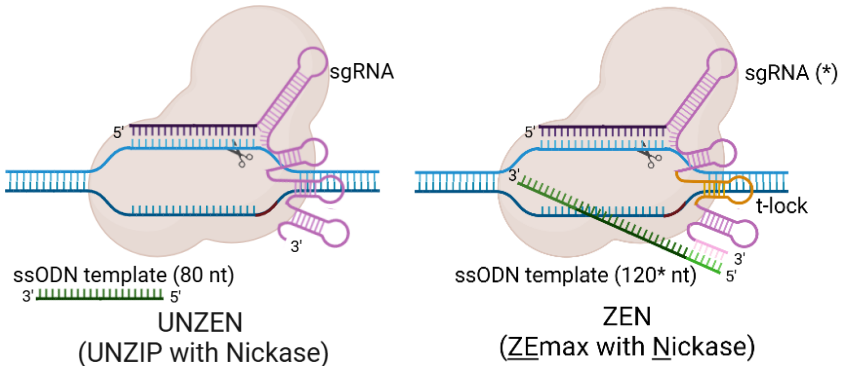
sgRNA
5'
3'
ssODN template (80 nt)
3' 5'
UNZEN
(UNZIP with Nickase)
sgRNA (*)
5'
3'
t-lock
3'
5'
ssODN template (120* nt)
ZEN
(ZEmax with Nickase)

b

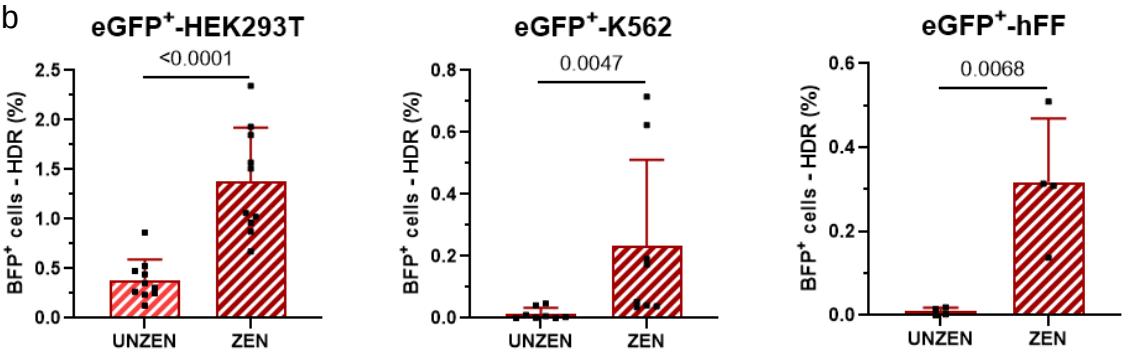
eGFP+-HEK293T
<0.0001
BFP+ cells - HDR (%)
2.5
2.0
1.5
1.0
0.5
0.0
UNZEN
ZEN
eGFP+-K562
0.0047
BFP+ cells - HDR (%)
0.8
0.6
0.4
0.2
0.0
UNZEN
ZEN
eGFP+-hFF
0.0068
BFP+ cells - HDR (%)
0.6
0.4
0.2
0.0
UNZEN
ZEN

c

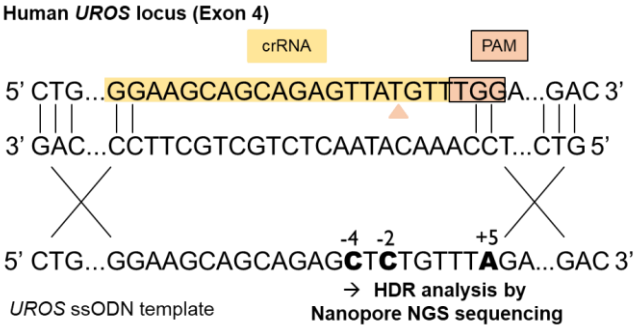
Human UROS locus (Exon 4)
crRNA
PAM
5' CTG...GGAAGCAGCAGAGTTATGTTTGGA...GAC 3'
3' GAC...CCTTCGTCGTCTCAATACAAACCT...CTG 5'
-4 -2 +5
5' CTG...GGAAGCAGCAGAGCTCTGTTTAGA...GAC 3'
→ HDR analysis by
Nanopore NGS sequencing
UROS ssODN template

d

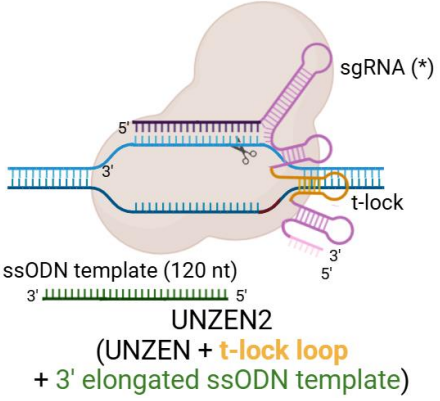
sgRNA (*)
5'
3'
t-lock
3'
5'
ssODN template (120 nt)
3' 5'
UNZEN2
(UNZEN + t-lock loop
+ 3' elongated ssODN template)

e

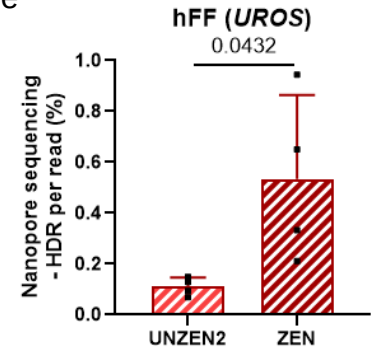
hFF (UROS)
0.0432
Nanopore sequencing
- HDR per read (%)
1.0
0.8
0.6
0.4
0.2
0.0
UNZEN2
ZEN

f

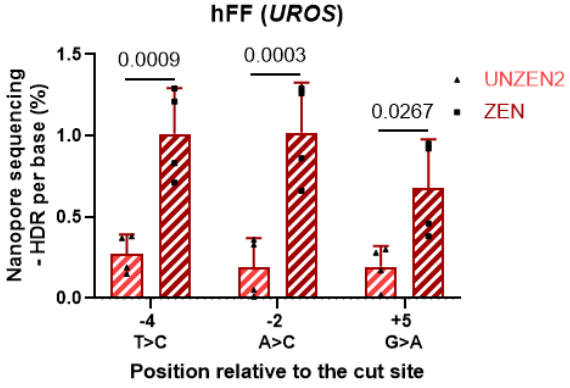
hFF (UROS)
Nanopore sequencing
- HDR per base (%)
1.5
1.0
0.5
0.0
0.0009
0.0003
0.0267
UNZEN2
ZEN
-4
T>C
-2
A>C
+5
G>A
Position relative to the cut site

Fig 4: Increased availability of HDR template with ZEN is essential to repair nicks by HDR. a Representation of RNPs “UNZEN (nickase Cas9 with free ssODN template) and “Zip Editing Nickase” (ZEN, nickase Cas9 with ssODN import using hybridization of 5’-elongated ssODN to the t-lock gRNA). **b** Flow cytometry quantification of the edition with nickase Cas9 with (ZEN) or without (UNZEN) the correction template physically bound to the gRNA in eGFP$^+$-HEK293T cells (n=10), eGFP$^+$-K562 cells (n=8), and eGFP$^+$-hFFs (n=4). The proportions of cells expressing BFP (HDR-edited) one week after transfection are reported. The mean ± SD is shown. Statistical significance determined by unpaired t-test (eGFP$^+$-HEK293T cells, eGFP$^+$-hFFs) or Mann-Whitney test (eGFP$^+$-K562 cells). **c** Editing strategy to edit *UROS* in hFFs. **d** Representation of “UNZEN2" system (control of ZEN with modified gRNA but without ssODN-gRNA annealing). **e** Nanopore sequencing to quantify HDR editing per read (total HDR, 3 modifications) with UNZEN2 or ZEN (n=4). The mean ± SD is shown. Statistical significance determined by unpaired t-test. **f** Nanopore sequencing to quantify HDR editing per base with UNZEN2 or ZEN (n=4). The mean ± SD is shown. Statistical significance determined by two-way ANOVA. Schemas created with BioRender.com.

Fig. 5

a

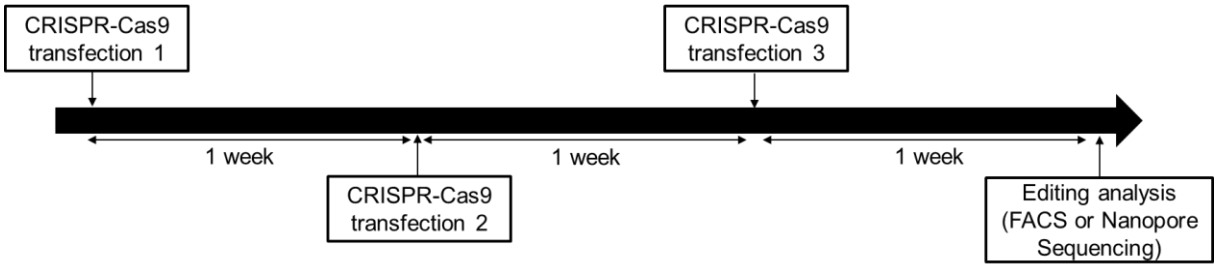
CRISPR-Cas9 transfection 1
CRISPR-Cas9 transfection 3
1 week
1 week
1 week
CRISPR-Cas9 transfection 2
Editing analysis (FACS or Nanopore Sequencing)

b

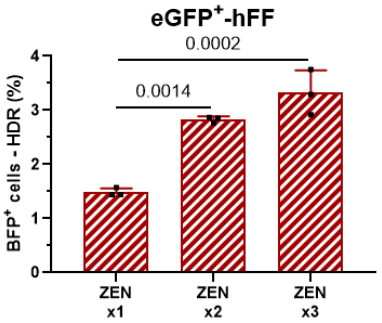
eGFP+-hFF
0.0002
0.0014
BFP+ cells - HDR (%)
0
1
2
3
4
ZEN x1
ZEN x2
ZEN x3

c

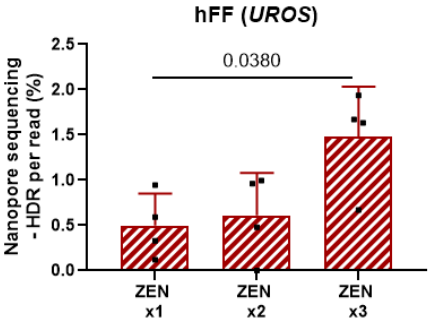
hFF (UROS)
0.0380
Nanopore sequencing - HDR per read (%)
0.0
0.5
1.0
1.5
2.0
2.5
ZEN x1
ZEN x2
ZEN x3

d

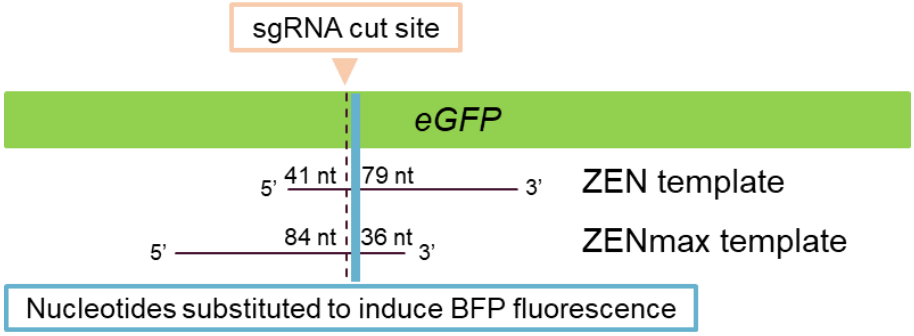
sgRNA cut site
eGFP
5'
41 nt
79 nt
3'
ZEN template
5'
84 nt
36 nt
3'
ZENmax template
Nucleotides substituted to induce BFP fluorescence

e

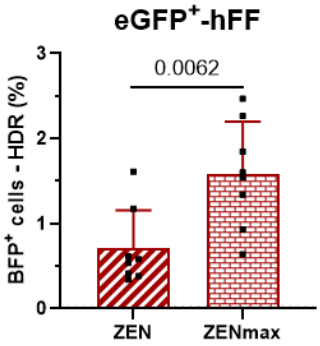
eGFP+-hFF
0.0062
BFP+ cells - HDR (%)
0
1
2
3
ZEN
ZENmax

f

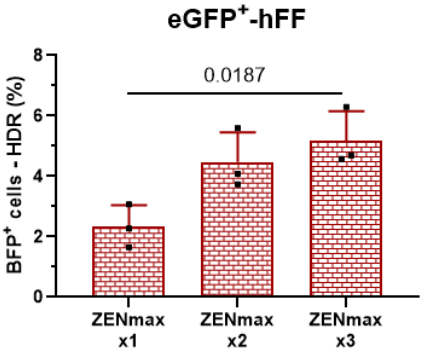
eGFP+-hFF
0.0187
BFP+ cells - HDR (%)
0
2
4
6
8
ZENmax x1
ZENmax x2
ZENmax x3

Fig. 5: Iterative editing and ssODN template design improve HDR editing with ZEN. a Timeline for iterative transfections (RNPs nucleofection). **b** Flow cytometry quantification of edition after 1, 2 or 3 transfection(s) with ZEN in eGFP$^+$-hFFs (n=3). The proportions of cells expressing BFP (HDR-edited) one week after transfection are reported. The mean ± SD is shown. Statistical significance determined by one-way ANOVA. **c** Nanopore sequencing quantification of edition after 1, 2 or 3 transfection(s) with ZEN in hFFs (n=4). Total HDR (3 modifications) rates per read are reported. The mean ± SD is shown. Statistical significance determined by one-way ANOVA. **d** Representation of BFP-ssODN template position relative to the cut site used for ZEN or ZENmax. **e** Flow cytometry quantification of edition with ZEN or ZENmax in eGFP$^+$-hFFs (n=8). The proportions of cells expressing BFP (HDR-edited) one week after transfection are reported. The mean ± SD is shown. Statistical significance determined by unpaired t-test. **f** Flow cytometry quantification of edition after 1, 2 or 3 transfection(s) with ZENmax in eGFP$^+$-hFFs (n=3). The proportions of cells expressing BFP (HDR-edited) one week after transfection are reported. The mean ± SD is shown. Statistical significance determined by one-way ANOVA.

Fig. 6

a

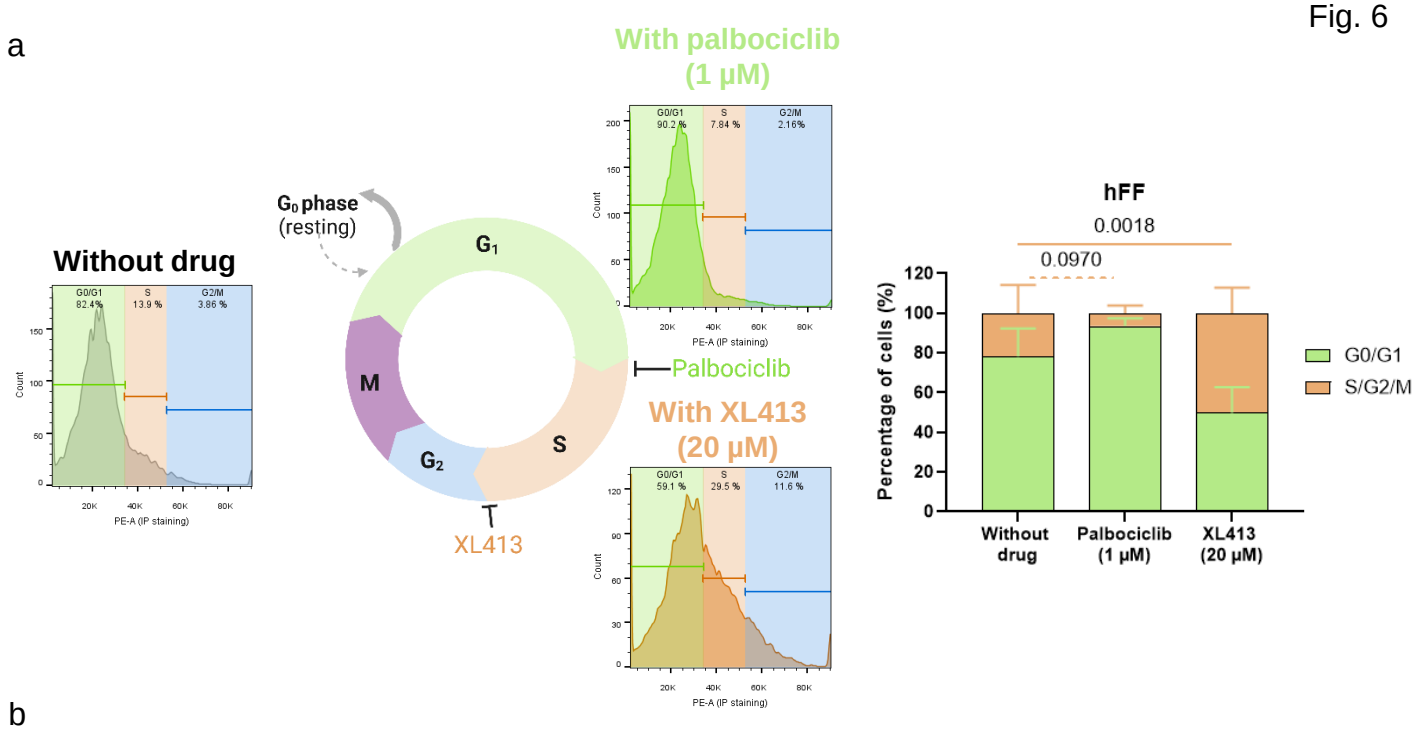
With palbociclib
(1 μM)
Without drug
G0/G1
82.4 %
S
13.9 %
G2/M
3.86 %
G0/G1
90.2 %
S
7.84 %
G2/M
2.16 %
G0/G1
59.1 %
S
29.5 %
G2/M
11.6 %
Count
PE-A (IP staining)
G0 phase
(resting)
G1
S
G2
M
Palbociclib
With XL413
(20 μM)
XL413
hFF
0.0018
0.0970
Percentage of cells (%)
G0/G1
S/G2/M
Without drug
Palbociclib (1 μM)
XL413 (20 μM)

b

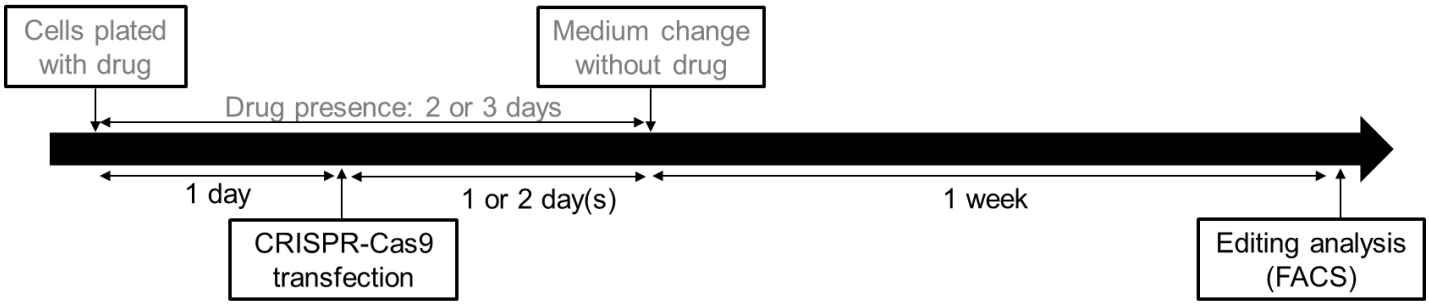
Cells plated with drug
Medium change without drug
Drug presence: 2 or 3 days
1 day
1 or 2 day(s)
1 week
CRISPR-Cas9 transfection
Editing analysis (FACS)

c

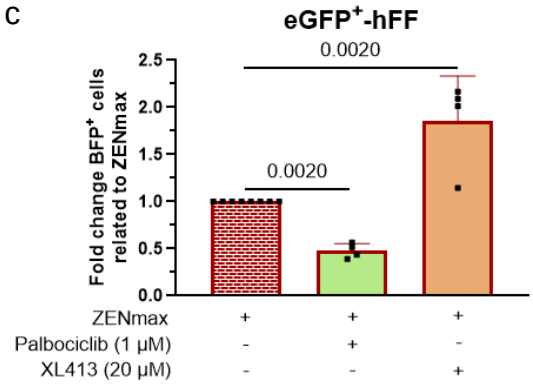
eGFP+-hFF
0.0020
0.0020
Fold change BFP+ cells related to ZENmax
ZENmax
Palbociclib (1 μM)
XL413 (20 μM)

d

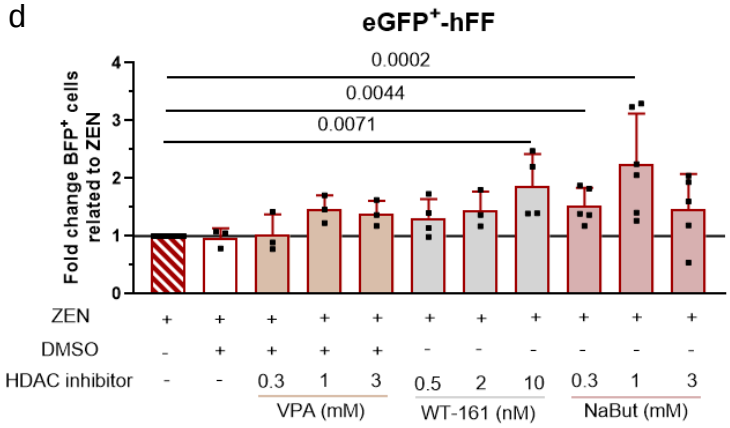
eGFP+-hFF
0.0002
0.0044
0.0071
Fold change BFP+ cells related to ZEN
ZEN
DMSO
HDAC inhibitor
VPA (mM)
WT-161 (nM)
NaBut (mM)

e

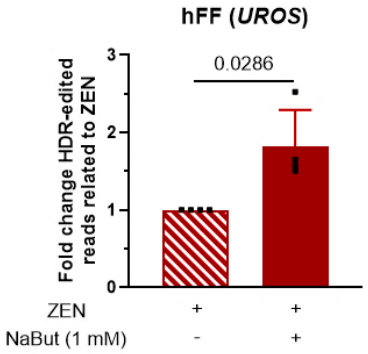
hFF (UROS)
0.0286
Fold change HDR-edited reads related to ZEN
ZEN
NaBut (1 mM)

Fig. 6: Modulation of 'cell state' can be associated with ZEN to increase HDR editing. a Illustrative cell cycle results of eGFP$^+$-hFFs with palbociclib, XL413 or without drug (left panel). Flow cytometry quantification of the proportion of eGFP$^+$-hFFs in G0/G1 or S/G2/M phases with palbociclib, XL413 or without drug (right panel, n=4). The mean ± SD is shown. Statistical significance to cells without drugs determined by two-way ANOVA. **b** Timeline for transfections (RNPs nucleofection) in presence of drugs. **c** Flow cytometry quantification of HDR edition with Cas9 nickase (ZENmax) with or without synchronization of eGFP$^+$-hFFs in G0/G1 phase with palbociclib or in S/G2/M phases with XL413 (n=4). The proportions of cells expressing BFP (HDR-edited) one week after transfection are reported. Fold changes indicate fold increases between conditions with or without drug. The mean ± SD is shown. Statistical significance to ZENmax without drugs determined by Kolmogorov-Smirnov test. **d** Flow cytometry quantification of HDR edition with nickase Cas9 (ZEN) with or without VPA (n=3), WT-161 (n=3) or NaBut (n=5) exposure. The proportion of cells expressing BFP (HDR-edited) one week after transfection is reported. Fold changes indicate fold increases between the conditions with either VPA, WT-161 or NaBut and the condition without drug. The mean ± SD is shown. Statistical significance determined by Kruskal-Wallis test. **d** Nanopore sequencing to quantify *UROS* HDR editing per read with nickase Cas9 (ZEN) with or without NaBut in hFFs (n=4). Fold changes indicate fold increases between the conditions with or without NaBut. The mean ± SD is shown. Statistical significance determined by Kolmogorov-Smirnov test. Schemas created with BioRender.com.

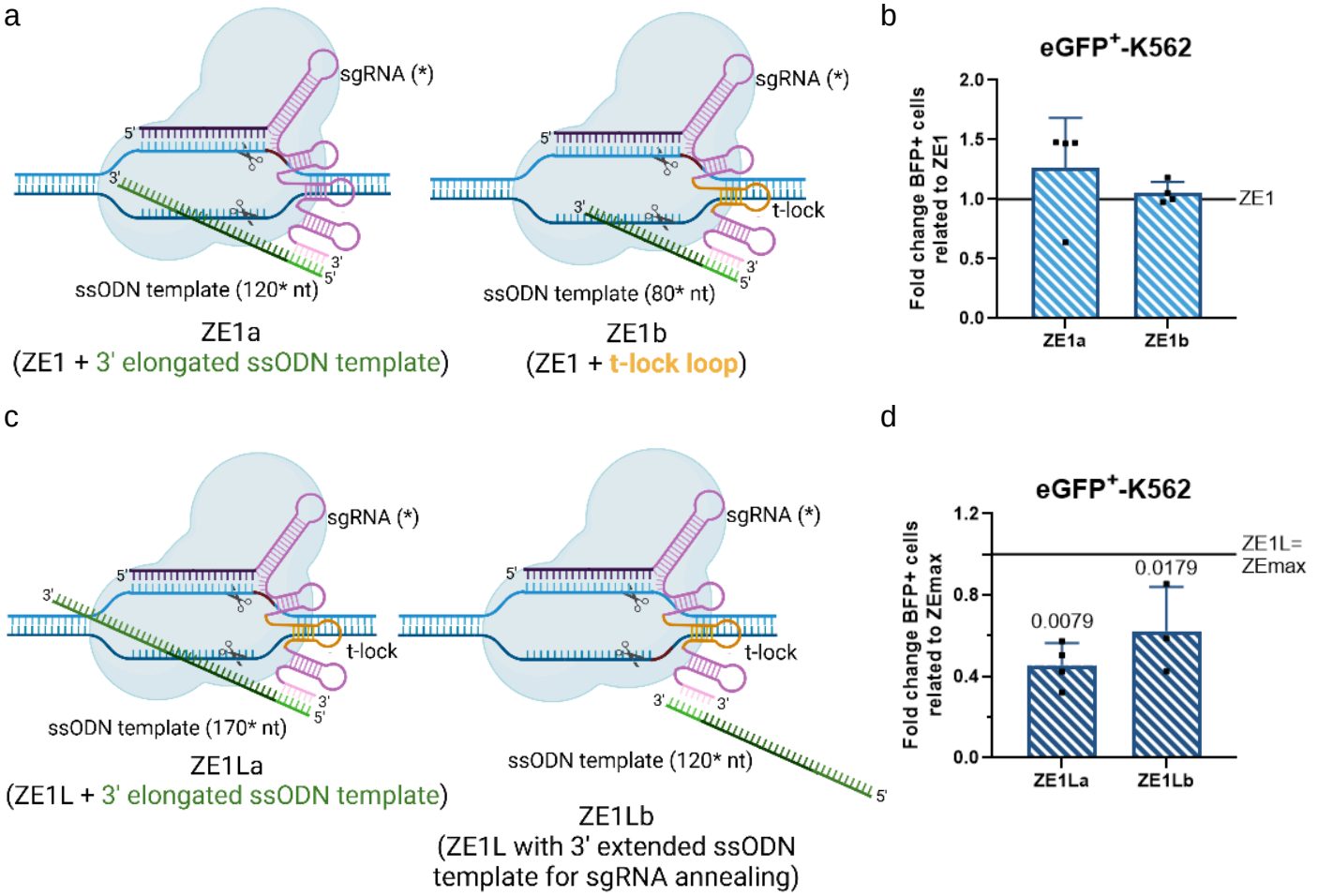

Supplementary Fig. 1: Zip Editing development. a Representation of RNPs used in the ZE1a (ZE1 with 3-'elongated ssODN template) and ZE1b (ZE1 with additive t-lock loop in the gRNA) import systems. **b** Flow cytometry quantification of HDR edition with nuclease Cas9 with ZE1a or ZE1b in eGFP$^+$-K562 cells (n=4). The proportions of cells expressing BFP (HDR-edited) one week after transfection are reported. Fold changes indicate fold increases between ZE1a or ZE1b relative to ZE1. The mean ± SD is shown. **c** Representation of RNPs used in the ZE1La (ZE1L with 3-'over-elongated ssODN template) and ZE1Lb (ZE1L with ssODN 3'-hybridization to the gRNA, instead of 5') import systems. **d** Flow cytometry quantification of HDR edition with nuclease Cas9 with ZE1La (n=4) and ZE1Lb (n=3) in eGFP$^+$-K562 cells. The proportions of cells expressing BFP (HDR-edited) one week after transfection are reported. Fold changes indicate fold increases between ZE1La or ZE1Lb relative to ZE1L. The mean ± SD is shown. Statistical significance to ZE1L determined by Kolmogorov-Smirnov test. Schemas created with BioRender.com.

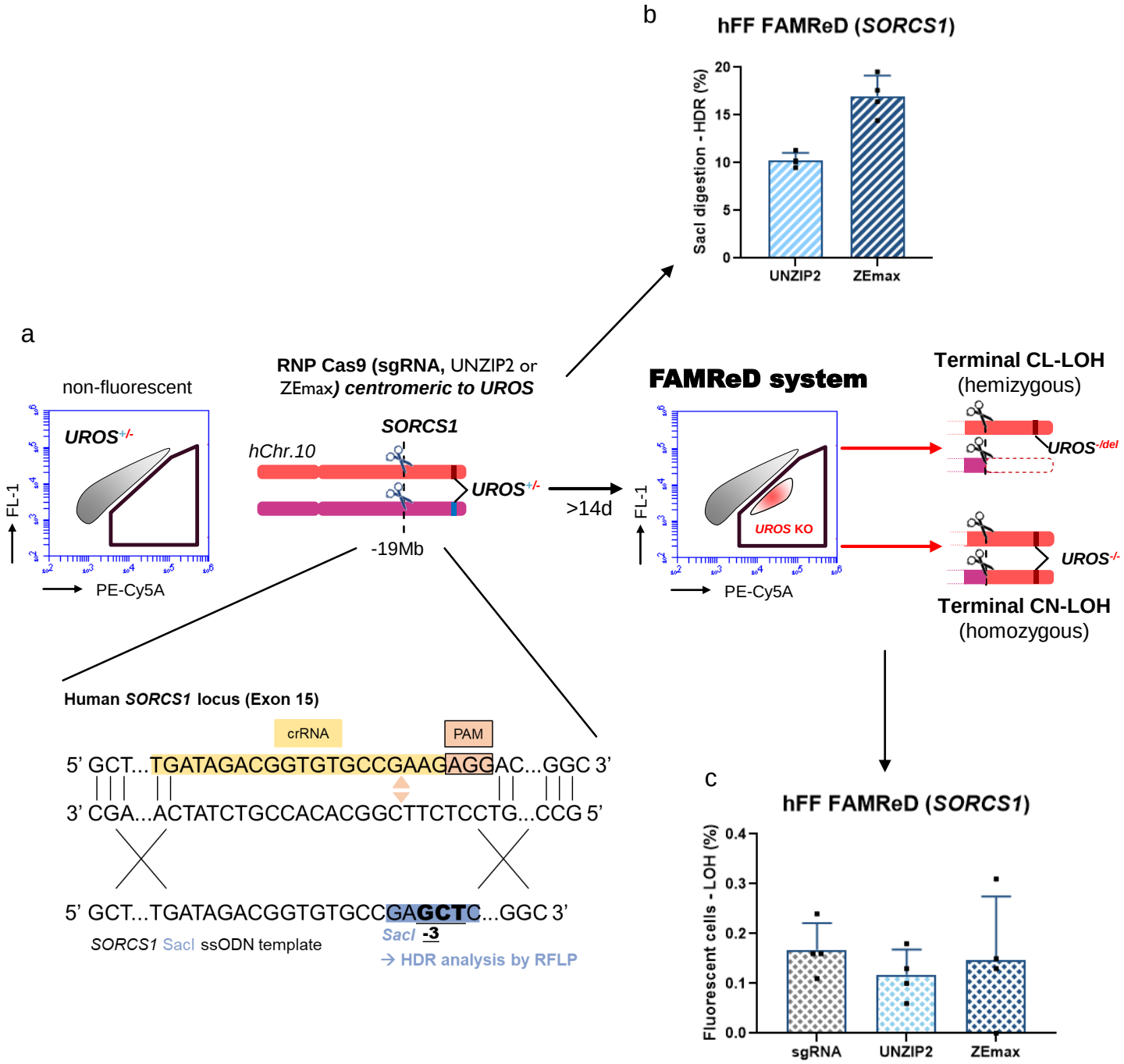

Supplementary Fig. 2: FAMReD technology to detect loss of heterozygosity (LOH) after CRISPR editing. a FAMReD system to detect and quantify LOH after CRISPR editing and editing strategy to edit *SORCS1* (insertion of *SacI* restriction site) in hFFs. **b** Capillary electrophoresis of *SacI* digestion products to quantify HDR editing with UNZIP2 or ZEmax (n=4). The mean ± SD is shown. **c** LOH quantification after CRISPR editing with sgRNA only, UNZIP2 or ZEmax (n=4). The mean ± SD is shown.

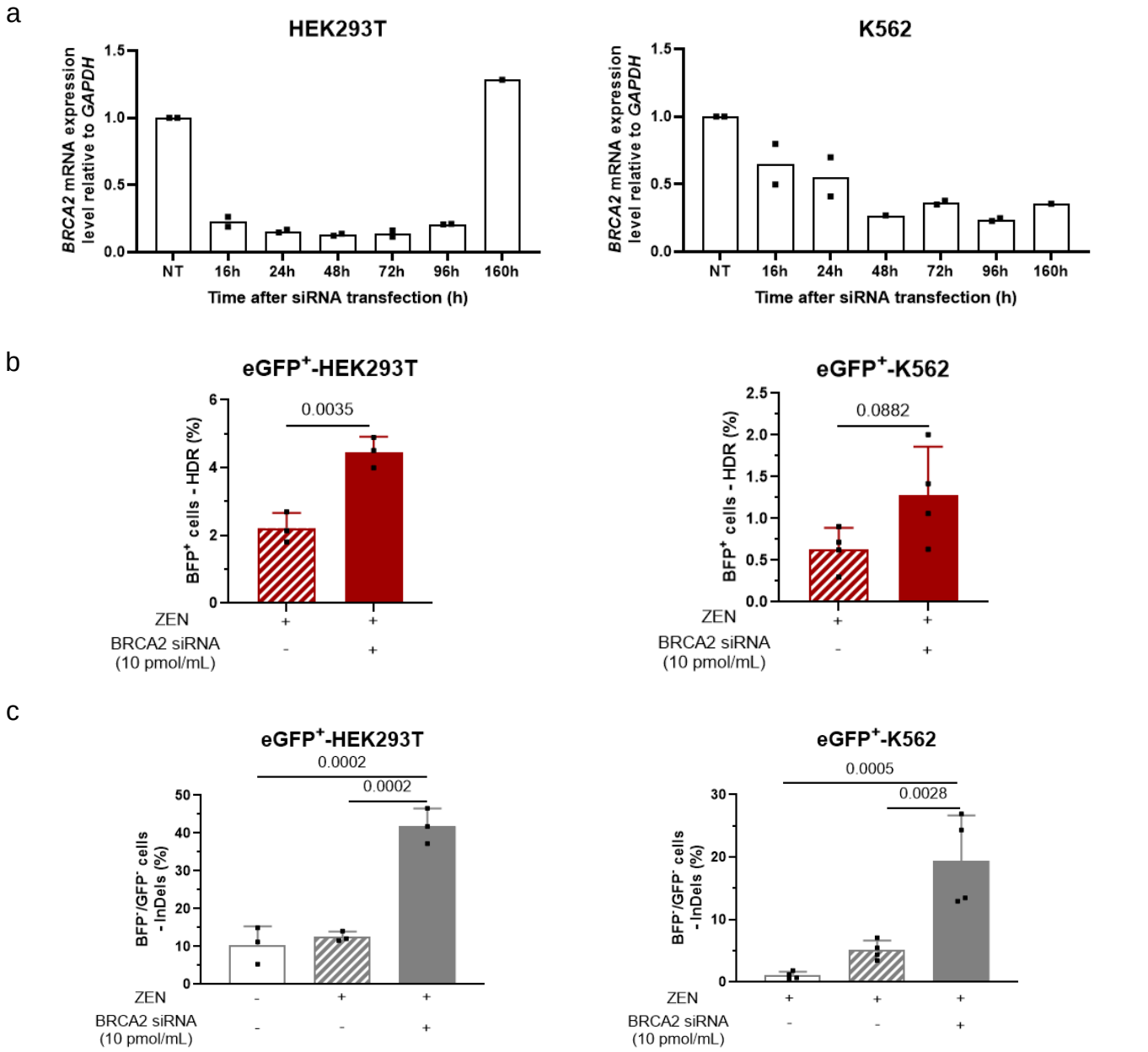

Supplementary Fig. 3: Modulation of DNA repair pathways can be associated with ZEN to increase HDR editing. a RTqPCR quantification of *BRCA2* mRNA expression levels over time after transfection of siRNA directed against *BRCA2* in HEK293T cells (left panel, n=2) or K562 cells (right panel, n=2). Values are normalized to *GAPDH* expression levels. The mean is shown. **b** Flow cytometry quantification of HDR edition with nickase Cas9 (ZEN) with or without inhibition of *BRCA2* by siRNA during edition in eGFP$^+$-HEK293T cells (left panel, n=3) or eGFP$^+$-K562 cells (right panel, n=4). The proportions of cells expressing BFP (HDR-edited) one week after transfection are reported. The mean ± SD is shown. Statistical significance determined by unpaired t-test. **c** Flow cytometry quantification of imprecise edition with nickase Cas9 (ZEN) with or without inhibition of *BRCA2* by siRNA in eGFP$^+$-HEK293T cells (left panel, n=3) or eGFP$^+$-K562 cells (right panel, n=4). The proportions of cells expressing neither BFP nor eGFP one week after transfection are reported. The mean ± SD is shown. Statistical significance determined by one-way ANOVA.

Supplementary Table 1: gRNA sequences for CRISPR-Cas9 editing.

sgRNA	Sequence (5' to 3')
sgRNA eGFP (UNZIP, UNZEN)	CTCGTGACCACCCTGACCTAGTTTTAGAGCTAGAAATAGCAAGTTAAAATAAGGCTAGTCCGTTATCAACTTGAAAAAGTGGCACCGAGTCGGTGCTTTT
sgRNA eGFP (ZE1, ZE1b)	CTCGTGACCACCCTGACCTAGTTTTAGAGCTAGAAATAGCAAGTTAAAATAAGGCTAGTCCGTTATCAACTTGAAAAAGTGGCACCGAGTCGGTGCTTTTCTGCCATCAAAGCGTGCTCAGTCT
sgRNA eGFP (ZE1a, ZE1D, ZE1La, ZE1Lb, ZEmax, ZEN, ZENmax)	CTCGTGACCACCCTGACCTAGTTTTAGAGCTAGAAATAGCAAGTTAAAATAAGGCTAGTCCGTTATCAACTTGGACTTCGGTCCAAGTGGCACCGAGTCGGTGCTTTTCTGCCATCAAAGCGTGCTCAGTCTGCTGCC
sgRNA HBB (UNZIP2, ZEmax)	GTAACGGCAGACTTCTCCTCGTTTTAGAGCTAGAAATAGCAAGTTAAAATAAGGCTAGTCCGTTATCAACTTGGACTTCGGTCCAAGTGGCACCGAGTCGGTGCTTTTCTGCCATCAAAGCGTGCTCAGTCTGCTGCC
sgRNA UROS (UNZIP2, ZEmax, UNZEN2, ZEN)	GGAAGCAGCAGAGTTATGTTGTTTTAGAGCTAGAAATAGCAAGTTAAAATAAGGCTAGTCCGTTATCAACTTGGACTTCGGTCCAAGTGGCACCGAGTCGGTGCTTTTCTGCCATCAAAGCGTGCTCAGTCTGCTGCC
sgRNA CFTR_G542X_modeling (UNZIP)	GACAATATAGTTCTTGGAGAGTTTTAGAGCTAGAAATAGCAAGTTAAAATAAGGCTAGTCCGTTATCAACTTGAAAAAGTGGCACCGAGTCGGTGCTTTT
sgRNA CFTR_G542X_modeling (ZEmax)	GACAATATAGTTCTTGGAGAGTTTTAGAGCTAGAAATAGCAAGTTAAAATAAGGCTAGTCCGTTATCAACTTGGACTTCGGTCCAAGTGGCACCGAGTCGGTGCTTTTCTGCCATCAAAGCGTGCTCATTCTGCCATCAAAGCGTGCTCA
sgRNA CFTR_G542X_correction (UNZIP2, ZEmax)	GACAATATAGTTCTTTGAGAGTTTTAGAGCTAGAAATAGCAAGTTAAAATAAGGCTAGTCCGTTATCAACTTGGACTTCGGTCCAAGTGGCACCGAGTCGGTGCTTTTCTGCCATCAAAGCGTGCTCAGTCTGCTGCC
sgRNA SORCS1 (UNZIP2, ZEmax)	TGATAGACGGTGTGCCGAAGGTTTTAGAGCTAGAAATAGCAAGTTAAAATAAGGCTAGTCCGTTATCAACTTGGACTTCGGTCCAAGTGGCACCGAGTCGGTGCTTTTCTGCCATCAAAGCGTGCTCAGTCTGCTGCC

Supplementary Table 2: HDR ssODN template sequences for CRISPR-Cas9 HDR editing.

HDR template	Sequence (5' to 3')
BFP (UNZIP, UNZEN)	AAGCTGCCCGTGCCCTGGCCCACCCTCGTGACCACCCTGAGCCACGGCGTGCAGTGCTTCGCCCGCTACCCCGACCACATGA
BFP (ZE1, ZE1a)	TGAGCACGCTTTGATGGCAGAAGCTGCCCGTGCCCTGGCCCACCCTCGTGACCACCCTGAGCCACGGCGTGCAGTGCTTCGCCCGCTACCCCGACCACAT
BFP (ZE1D) 1/2	GGCAGCAGACTGAGCAAGCTGCCCGTGCCCTGGCCCACCCTCGTGACCACCCTGAGCCACGGCGTGCAGTGCTTCGCCCGCTACCCCGACCACAT
BFP (ZE1D) 2/2	ACGCTTTGATGGCAGAAGCTGCCCGTGCCCTGGCCCACCCTCGTGACCACCCTGAGCCACGGCGTGCAGTGCTTCGCCCGCTACCCCGACCACAT
BFP (ZE1b, ZEmax, ZEN)	GGCAGCAGACTGAGCACGCTTTGATGGCAGAAGCTGCCCGTGCCCTGGCCCACCCTCGTGACCACCCTGAGCCACGGCGTGCAGTGCTTCGCCCGCTACCCCGACCACATGAAGCAGCACGACTTCTTCAAGTCCGCCATGCCCGAAGGC
BFP (ZE1La)	TGAGCACGCTTTGATGGCAGAAGCTGCCCGTGCCCTGGCCCACCCTCGTGACCACCCTGAGCCACGGCGTGCAGTGCTTCGCCCGCTACCCCGACCACATGAAGCAGCACGACTTCTTCAAGTCCGCCATGCCCGAAGGCTACGTCCAGGAGCGCACCATCTTCTTCAAGGACGACGGCACCTACAAGAC
BFP (ZE1Lb)	AAGCTGCCCGTGCCCTGGCCCACCCTCGTGACCACCCTGAGCCACGGCGTGCAGTGCTTCGCCCGCTACCCCGACCACATGAAGCAGCACGACTTCTTCAAGTCCGCCATGCCCGAAGGCTGAGCACGCTTTGATGGCAG
BFP (ZENmax)	GGCAGCAGACTGAGCACGCTTTGATGGCAGCACCTACGGCAAGCTGACCCTGAAGTTCATCTGCACCACCGGCAAGCTGCCCGTGCCCTGGCCCACCCTCGTGACCACCCTGAGCCACGGCGTGCAGTGCTTCGCCCGCTACCCCGACCA
HBB (UNZIP2)	TGACACAACTGTGTTCACTAGCAACCTCAAACAGACACCATGGTGCATCTGACTCCCGAGGAAAAATCCGCAGTCACTGCCCTGTGGGGCAAGGTGAACGTGGATGAAGTTGGTGGTGAG
HBB (ZEmax)	GGCAGCAGACTGAGCACGCTTTGATGGCAGTGACACAACTGTGTTCACTAGCAACCTCAAACAGACACCATGGTGCATCTGACTCCCGAGGAAAAATCCGCAGTCACTGCCCTGTGGGGCAAGGTGAACGTGGATGAAGTTGGTGGTGAG
UROS (UNZIP2, UNZEN2)	CTGAAGATTACGGGGGACTCATTTTTACCAGCCCCAGAGCAGTGGAAGCAGCAGAGCTCTGTTTAGAGCAAAACAATAAAACTGAAGGTGAGGGTGGGTCTGCTGTGGATTCCACTGGAC
UROS (ZEmax, ZEN)	GGCAGCAGACTGAGCACGCTTTGATGGCAGCTGAAGATTACGGGGGACTCATTTTTACCAGCCCCAGAGCAGTGGAAGCAGCAGAGCTCTGTTTAGAGCAAAACAATAAAACTGAAGGTGAGGGTGGGTCTGCTGTGGATTCCACTGGAC
CFTR_G542X_ modeling (UNZIP)	ACATCTCCAAGTTTGCAGAGAAAGACAATATAGTTCTTTAGGAGCTCGGAATCACACTGAGTGGAGGTCAACGAGCAAGA
CFTR_G542X_ modeling (ZEmax)	TGAGCACGCTTTGATGGCAGAATTTTCTATTTTTGGTAATAGGACATCTCCAAGTTTGCAGAGAAAGACAATATAGTTTAGGAGCTCGGAATCACACTGAGTGGAGGTCAACGAGCAAGAATTTCTTTAGCAAGGTGAAT
CFTR_G542X_ correction (UNZIP2)	TTCTATTTTTGGTAATAGGACATCTCCAAGTTTGCAGAGAAAGATAACATCGTCCTCGGAGAGGGTGGAATCACACTGAGTGGAGGTCAACGAGCAAGAATTTCTTTAGCAAGGTGAATA
CFTR_G542X_ correction (ZEmax)	GGCAGCAGACTGAGCACGCTTTGATGGCAGTTCTATTTTTGGTAATAGGACATCTCCAAGTTTGCAGAGAAAGATAACATCGTCCTCGGAGAGGGTGGAATCACACTGAGTGGAGGTCAACGAGCAAGAATTTCTTTAGCAAGGTGAATA
SORCS1 (UNZIP2)	GCTCTGAATGGCAGCTGGTCAAAGTAGATTACAAGTCCATTTTTGATAGACGGTGTGCCGAGCTCTACAGACCTTGGCAGCTGCACAGCCAGGTAGGAGGAAAAGAACTGAGACTAAGGC
SORCS1 (ZEmax)	GGCAGCAGACTGAGCACGCTTTGATGGCAGGCTCTGAATGGCAGCTGGTCAAAGTAGATTACAAGTCCATTTTTGATAGACGGTGTGCCGAGCTCTACAGACCTTGGCAGCTGCACAGCCAGGTAGGAGGAAAAGAACTGAGACTAAGGC

Supplementary Table 3: PCR primer sequences.

PCR primers	Sequence (5' to 3')
HBB_424pb_F	CTGATGGTATGGGGCCAAGAG
HBB_424pb_R	GTCTCCACATGCCCAGTTTCT
UROS_405pb_F (RFLP analysis)	TAGTTCCAGGCACATAGTAAGCAC
UROS_405pb_R (RFLP analysis)	TCCCAAGGCAGAGTCTGTGA
UROS_1kb_F (Nanopore sequencing)	CTCTAATCCCAGGCTGCGTC
UROS_1kb_R (Nanopore sequencing)	GCCTCCGCTCATCAGTGTAA
CFTR_415pb_F (RFLP analysis)	CAGCAATGTTGTTTTTGACCAACT
CFTR_415pb_R (RFLP analysis)	ACCCACTAGCCATAAAACCCC
CFTR_1kb_F (Nanopore sequencing)	AGGTCGTGAGAATGAGGTGC
CFTR_1kb_R (Nanopore sequencing)	TGGAGTGGCAGGGTCTATGA
SORCS1_484pb_F	TGAACGCCCCACAAATGCTC
SORCS1_484pb_R	TTGGATCTGAGTGCTGAACTGG

Supplementary Table 4: RTqPCR primer sequences.

RTqPCR primers	Sequence (5' to 3')
BRCA2_RTqPCR_F	CCAAGTGGTCCACCCCAAC
BRCA2_RTqPCR_R	GGCTGAGACAGGTGTGGAAA
GAPDH_RTqPCR_F	CTGCACCACCAACTGCTTAG
GAPDH_RTqPCR_R	AGGTCCACCACTGACACGTT